Pictet et al. Swiss Journal of Geosciences (2023) 116:1
https://doi.org/10.1186/s00015-022-00430-z

Swiss Journal of Geosciences

ORIGINAL PAPER

Open Access

Record of a dense succession of drowning phases in the Alpstein mountains, northeastern Switzerland: Part II—the Lower Cretaceous Schrattenkalk Formation (late Barremian)

Antoine Pictet[1*], Karl Tschanz[2] and Peter Kürsteiner[3]

Abstract

The Schrattenkalk Formation represents a complete succession of Lower Cretaceous shallow-water carbonate platform series cropping out in the Alpstein massif of north-eastern Switzerland. The Schrattenkalk Formation is traditionally divided into two sedimentary units, the "Lower" and the "Upper" Schrattenkalk, separated by the more marly Rawil Member. The "Lower" Schrattenkalk is habitually dated to the late Barremian, while the Rawil Member and the "Upper" Schrattenkalk are dated to the early Aptian. New field observations, however, call the lithostratigraphic dichotomy of the Schrattenkalk into question, as the neritic carbonates are disrupted by several key surfaces associated with karstic episodes and/or transgressive sediments, corresponding to ammonite-rich hemipelagic deposits on the distal shelf. A large number of ammonites were collected in the Drusberg Member as well as rare ammonites from the Schrattenkalk Formation. These ammonites as well as the neritic macrofauna from the Schrattenkalk Formation allow a precise dating of the onset of the Schrattenkalk Formation across the Alpstein massif and its successive phases of progradation. Three successive carbonate bodies and a fourth sedimentary intermediate rock body at the top of the Schrattenkalk platform are defined, based on new biostratigraphic data and updated interpretations of the sequence stratigraphy and geochemical data. The data shows a progressive onset of the Schrattenkalk carbonate platform along the studied transect, following a SE progradation over time. The oldest deposits refer to the upper Barremian *T. vandenheckii* Zone and the youngest carbonates to the uppermost Barremian *M. sarasini* Subzone. The new dating of the discontinuity surfaces and key-beds highlight three successive flooding events. The first drowning phase, which correlates with the "Sartousiana" event, dates from the middle late Barremian (upper *T. vandenheckii*—lower *G. sartousiana* Zone). The second phase, represented by the Rawil Member, is an incipient drowning, which seems to coincide with the latest Barremian Taxy event (usually reported to the *I. giraudi* and lowermost *M. sarasini* zones) according to rare ammonite discoveries. The final demise of the Schrattenkalk platform, situated close to the Barremian-Aptian boundary, is related to an exposure and consecutive drowning event.

Keywords Helvetic domain, Säntis nappe, Biostratigraphy, Sedimentology, Schrattenkalk, Barremian

Editorial handling: Wilfried Winkler

*Correspondence:
Antoine Pictet
antoine.pictet@unil.ch
[1] Musée Cantonal de Géologie, 1015 Lausanne, Switzerland
[2] Paläontologisches Institut und Museum, Universität Zürich, Karl-Schmid-Strasse 4, 8006 Zurich, Switzerland
[3] Naturmuseum St. Gallen, Rorschacherstrasse 263, 9016 St. Gallen, Switzerland

1 Introduction

The Schrattenkalk limestone, a landscaping element of the Helvetic realm, represents the most imposing lithostratigraphic unit of the Lower Cretaceous Helvetic series. It marks the panorama by its high and white rock walls and its large-scale lapies (karst topography). However, its establishment and evolution are subject of various chronostratigraphic and sedimentological models that are profoundly conflictual. The lithostratigraphic subdivision of the Schrattenkalk Formation has likewise been very fluctuant since the beginning of its investigation.

The Barremian time interval and more particularly the late Barremian-earliest Aptian is considered to have been a period of relative quietness in the evolution of the biosphere (Föllmi, 2012). This period is nested between the latest Hauterivian Faraoni episode (Cecca et al., 1994), the first widely recognized oceanic anoxic event of the Cretaceous and the Selli episode (Coccioni et al., 2003), one of the major phases of paleoenvironmental change of the entire Cretaceous (Föllmi, 2012). The apparent stability within this time-period is argued by lower rates of organic-matter preservation in the oceans and by the maximum extension of the Urgonian carbonate platform on the northern Tethyan margin (Föllmi, 2012). However, the occurrence of numerous thin laminated organic-rich muds (LOM) intervals is known from Barremian sediments of the Tethys (Aguado et al., 2014; Bersezio et al., 2002; Coccioni et al., 1998, 2003, 2006; Föllmi, 2012; Mahanipour & Eftekhari, 2017; Masse & Machhour, 1998; Weissert et al., 1979; Yilmaz et al., 2012) and in the Lower Saxony Basin (Malkoč & Mutterlose, 2010; Mutterlose & Böckel, 1998; Mutterlose & Bornemann, 2000; Mutterlose et al., 2003, 2009, 2010; Pauly et al., 2013). These black shales have been found in abundance in upper lower and lower upper Barremian sedimentary rocks and around the "Barremian/Aptian boundary" interval (Coccioni et al., 2003; Föllmi, 2012; Rieber, 1977; Sprovieri et al., 2006; Talbi et al., 2021; Weissert et al., 1979). Recent studies revised the age of the peri-Vocontian urgonian platforms (Frau et al., 2018a, 2020; Pictet et al., 2019, 2022; Tendil et al., 2018), permitting a better time calibration between neritic carbonate platforms and basinal sedimentary series. Based on these studies, a better synchronicity and timing between platform drownings and anoxic events is enabled.

Oceanic carbonates play a key role in the global carbon cycle as they represent the most important carbon sink (Wissler et al., 2003). In contrast, shallow-water carbonate platforms are particularly sensitive to environmental and oceanographic change (Föllmi et al., 2006, 2007; Wissler et al., 2003). A large amount of work has been dedicated to the Barremian to lowermost Aptian neritic carbonate succession deposited on the Helvetic domain of the north-western Tethyan shelf and more specifically to the sedimentological features of the Schrattenkalk platform due to its well exposed sections (e.g., Bonvallet, 2015; Bonvallet et al., 2019; Briegel, 1972; Burckhardt, 1896; Fichter, 1934; Funk & Briegel, 1979; Heim, 1905; Heim & Baumberger, 1933; Jost-Stauffer, 1993; Kempf, 1966; Lienert, 1965; Staeger, 1944; Wissler, 2001; Wissler et al., 2003). The Schrattenkalk Formation appears to be interspersed with several key surfaces associated to specific orbitolinids- and other fossils-bearing beds (Wissler et al., 2003) and to phosphate-bearing beds onto the platform slope (Bodin et al., 2006a, 2006b; Bonvallet et al., 2019; Föllmi & Gainon, 2008; Pictet et al., 2022; Wissler et al., 2003). Marine phosphate-bearing beds are commonly regarded as the result of drowning episodes. These were associated with increased nutrient input as consequence of intensified chemical weathering on the continent due to warmer and more humid climate conditions (Föllmi et al., 2007). These may coincide in time with large scale changes in the ocean-climate system likely related to increased submarine volcanic activity of the Ontong-Java Plateau, which eventually led to the worldwide early Aptian Selli episode (OAE1a; Coccioni et al., 2003; Erba et al., 2015; Föllmi, 2012).

The current study presents a new biostratigraphical and sedimentological model of the Schrattenkalk Formation in the Alpstein massif. This model is discussed in terms of episodes of environmental change affecting the north western Tethys margin and the associated oceanic anoxic event intervals and other laminated, organic rich muds (LOMs) of latest Barremian age.

2 Geographical and geological setting

The Alpstein massif, situated in north eastern Switzerland, is shared by the cantons of Appenzell Ausserrhoden, Appenzell Innerrhoden, and St.Gallen. The mountain range is located in the north-eastern part of the Helvetic nappes of Switzerland (Fig. 1A). The massif has been thrusted and folded in a north western direction during the Alpine orogenesis (Fig. 1B–D) and detached from its Jurassic substratum along the Säntis Thrust (Pfiffner, 1981). The Cretaceous record presents a well exposed and developed Barremian sedimentary succession composed of a shallow-water carbonate platform series (Urgonian facies) referred as Schrattenkalk Formation, prograding on hemipelagic slope deposits of the Tierwis Formation (Fig. 1B, C; see Pictet et al., 2022).

The delimitation of the hemipelagic limestone and marlstone alternations of the Drusberg Member (i.e., = upper part of the Tierwis Formation) from the neritic carbonates of the Schrattenkalk is problematic due to lateral and temporal transitions from one unit into the other (Bollinger, 1988; Schenk, 1992). The delimitation becomes even more progressive and blurred in the distal domain of the sedimentation area (i.e., further to the southeast; Bollinger, 1988; Heim & Baumberger, 1933). Heim, (1910–1916) already emphasises that the "Drusberg Layers" should be regarded solely as a division based on facies whose "boundary" fluctuates wildly and

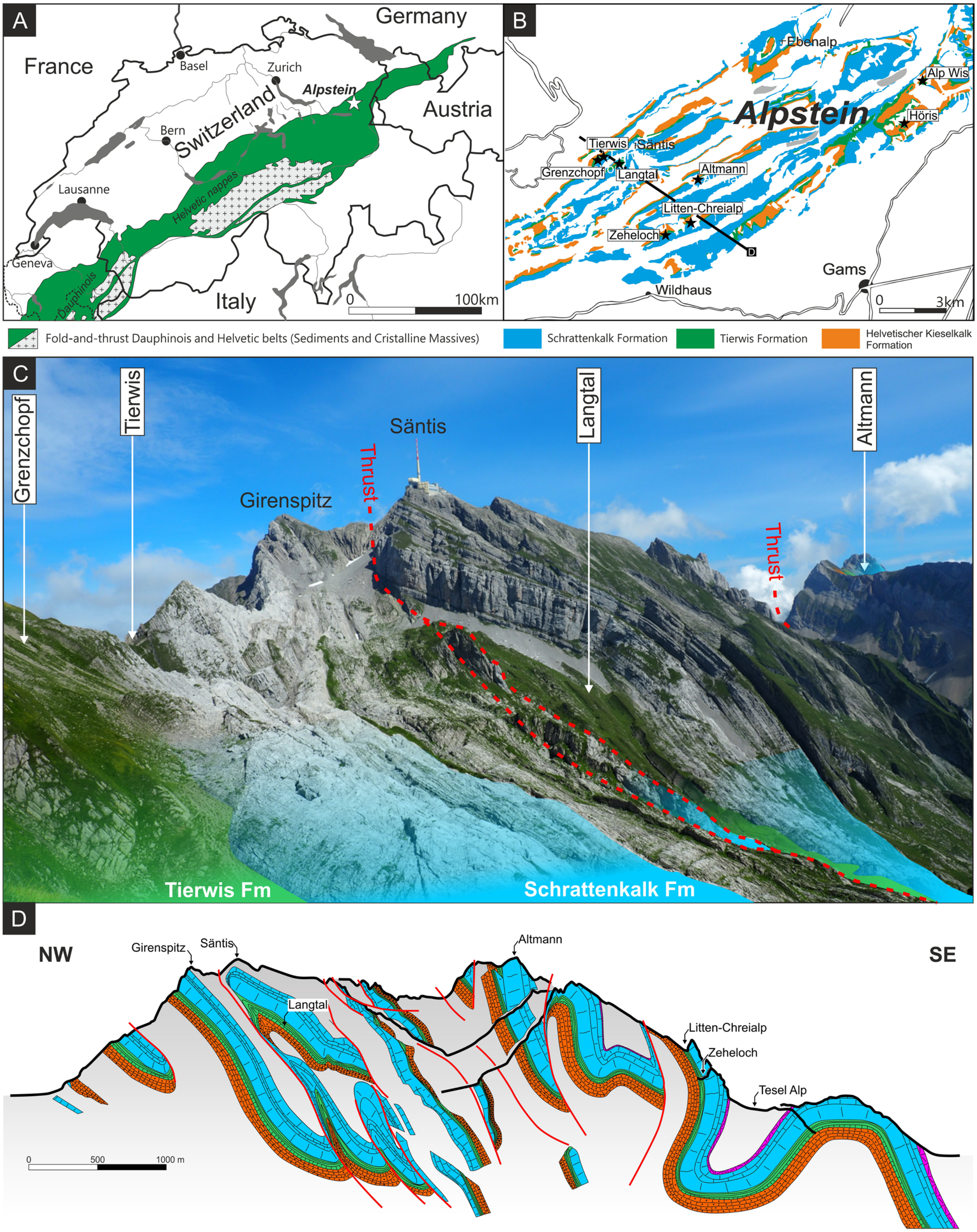

Fig. 1 **A** Location of the Alpstein massif of the Helvetic realm, simplified from Bodin et al. (2006a). **B** Simplified geological map with the location of the studied outcrops (modified after Eugster et al., 1982) with position of the cross-section illustrated in (**D**). **C** View of the Säntis part of the Alpstein massif with the position of some outcrops and the main thrust faults. **D** Geological cross-section of the Alpstein massif modified after Kempf (1966). The colours refer to (**B**), the S4-Gr unit is shown in purple

stratigraphically rises to the south. Nevertheless, the ecological relationship between the Schrattenkalk and the Drusberg series is clear. The Schrattenkalk limestone represents a neritic sedimentary succession passing seaward to the hemipelagic slope deposits of the "Drusberg layers" (Funk & Briegel, 1979; Heim, 1910–1916).

The "Schratten-Kalk" was mentioned for the first time by Studer (1834) describing the vast limestone fields of the southern slopes of the Schrattenflue Mountain (Canton Lucerne, Switzerland, Fig. 2). The Schrattenflue itself draws the origin of its name from the local language in which "schratten" means lapies (karst plateau). The Schrattenkalk term was popularized in the whole Helvetic domain by Heim, (1910–1916), prevailing on the French Urgonian limestone of d'Orbigny, (1847–1849) (see Funk & Briegel, 1979; Schenk, 1992). Funk and Briegel (1979) raised the question of whether it is permissible to compare the Schrattenkalk with the French Urgonian Formation. Following the definition worked out by the Colloquium on the Lower Cretaceous (Rat, 1965), the urgonian denomination is restricted to Lower Cretaceous limestone facies, which contain rudist shells of the genus *Toucasia* Munier-Chalmas, 1873. Such a definition allows equivalence between the Urgonian Formation and the Schrattenkalk Formation. The "Schrattenkalk series" were originally subdivided by Kaufmann (1867) into two units, which share nothing with their current lithostratigraphic nomenclature (Fig. 2). Nowadays, the Schrattenkalk Formation is conventionally subdivided into a "Lower Schrattenkalk" unit and an "Upper Schrattenkalk" unit sensu Heim, (1910–1916; i.e., = lower and upper rudists-bearing limestone of Kaufmann, 1867; Fig. 2), separated by the "Orbitulina Beds" (Kaufmann, 1867) or "Lower Orbitulina Beds" (Burckhardt, 1896), today referred as Rawil Member.

These "Orbitulina Beds" were reported for the first time by Kaufmann (1867) at the locality of Lopperberg (Canton of Nidwalden) where he described an intercalated marly bundle inside the Schrattenkalk series (Fig. 2). This intercalation is characterised by blue to yellow, iron-rich, sandy marlstones and limestones, which he named "Lower Orbitulina Beds" due to the mass occurrence of the benthic foraminifera *Palorbitolina lenticularis* (Blumenbach, 1805). Lienert (1965) designated these layers in the Säntis area as "Middle Schrattenkalk". Schenk (1992) described the presence of abundant plant remains such as wood fragments. She introduced the Rawil Member to define the Lower Orbitolina Beds from the Wildhorn nappe of the Bernese Oberland, which represent more distal environments of the Helvetic domain compared to the Lower Orbitolina Beds type-series of central and eastern Switzerland. The Rawil Member and the Lower Orbitolina Beds are considered to be largely synchronous due to their microfaunal association (Lienert, 1965). The geographic distribution of the Rawil Member and the Lower Orbitolina Beds is limited to the proximal platform. A dichotomy of the Schrattenkalk series seems therefore only possible in this domain.

Briegel (1972) formally defined the Schrattenkalk series as a formation (Fig. 2). Bollinger (1988) divided the Schrattenkalk Formation in ascending order in a Schrattenkalk Member and a Grünten Member (Bollinger, 1988; the latter corresponding to the Upper Orbitolina Beds; Burckhardt, 1896; Fichter, 1934). Nevertheless, the glauconitic echinodermic series of the Grünten Member are considered as devoid of rudist shells and contains

Studer (1834)	Kaufmann (1867)		Burckhardt (1896)		Heim (1910-1916, 1919)
				Oberer Orbitulinaschichten	Echinodermenbreccie - Grüntenschichten
Schratten-Kalk	Oberes Urgonien Rudistenkalk	Oberer Rudistenkalk	Oberes Urgonien Rudistenkalk	Oberer Requienienkalk	Obere(r) Schrattenkalk
		Orbitulinaschichten		Untere Orbitulinaschichten	Orbitolinenmergel
		Unterer Rudistenkalk		Unterer Requienienkalk	Untere(r) Schrattenkalk
	Unteres Urgonien		Unteres Urgonien		

Briegel (1971)		Bollinger (1988)			Schenk (1992)		Funk (1993)		Linder et al. (2006) & Föllmi et al. (2006, 2007)	
			Grünten Member			Oberer Orbitolinenschichten			Gars. Fm	Grünten Member
Schrattenkalk-formation	Obere Schrattenkalk	Schrattenkalk Formation	Schrattenkalk Mb		Schrattenkalk Formation	Oberer Schrattenkalk	Schrattenkalk Formation	Upper Schrattenkalk	Schrattenkalk Formation	Upper Schrattenkalk
	Obere Hurstmergel			Orbitolinenschichten		Untere Orbitolinenschichten (*p.p.* = Rawil Member)		Lower Orbitolina Beds		Lower Orbitolina Beds / Rawil Member
	Untere Schrattenkalk / Untere Hurstmergel					Unterer Schrattenkalk		Lower Schrattenkalk		Lower Schrattenkalk

Fig. 2 Summary table of the various historical terminologies used for the Schrattenkalk Formation and members

phosphatic beds. It does not fit the definition of the Urgonian facies accepted by the Colloquium on the Lower Cretaceous (Rat, 1965). Thus, the Grünten Member was moved to the base of the overlying Garschella Formation by Linder et al. (2006) (Fig. 2). Funk et al. (1993) introduced the Lower and Upper Schrattenkalk members to name the two superposed cliffs constituting the formation (Fig. 2). Föllmi et al. (2007) extended the Rawil Member to the whole Helvetic domain, replacing the Lower Orbitolina Beds type-series of central and eastern Switzerland (Fig. 2).

The establishment and evolution of the Schrattenkalk platform are subject of various chronostratigraphic and sedimentological models. Until recently the dating of the Schrattenkalk Formation was mainly based on the neritic foraminifera biostratigraphy of the family Orbitolinidae (Lienert, 1965; Schroeder et al., 1968, 2002, 2007). The use of these neritic microfossils led to profoundly conflictual chronostratigraphic datings of the Schrattenkalk Formation [Fig. 3; e.g., Clavel et al., 2014 versus Bonvallet et al. (2019), as well as Schroeder et al. (2007) versus Föllmi, (2008)]. Platform-to-basin correlations as well as correlations between mountain ranges of the Helvetic/Dauphinois domain were also used to date indirectly the Schrattenkalk Formation [e.g., Bodin et al., (2006a, 2006b) versus Clavel et al., (2014)]. A peculiarly condensed bed, called Chopf Bed by Briegel (1972), was identified in the Drusberg Member in Vorarlberg (Bollinger, 1988; Heim & Baumberger, 1933), in eastern Switzerland (Bodin et al., 2006a, 2006b; Briegel, 1972; Heim, 1910–1916; Lienert, 1965; Oberholzer, 1933; Pictet et al., 2022; Wissler et al., 2003) and in central Switzerland (Fichter, 1934; Staeger, 1944). Bodin et al. (2006a) dated the Chopf Bed in its type locality as transitional between

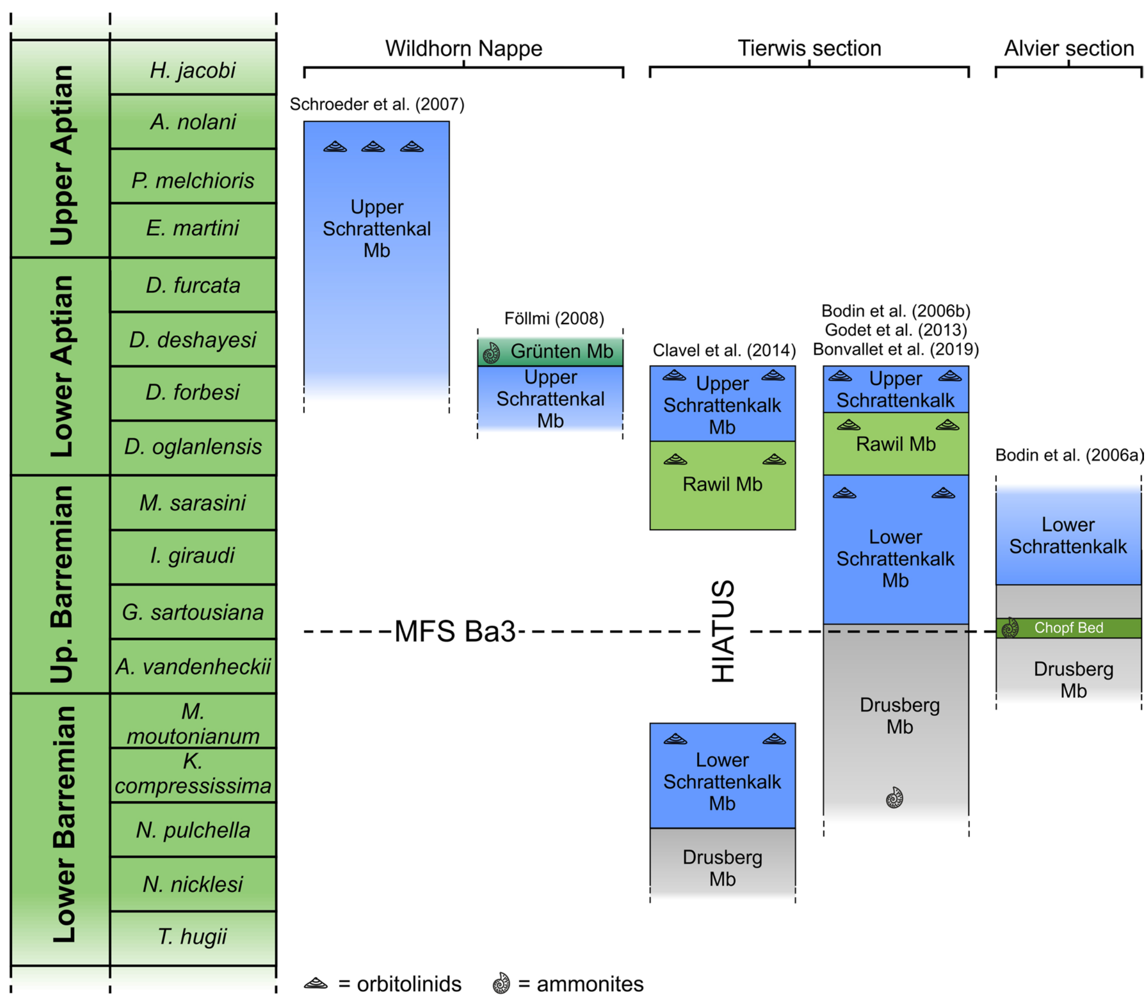

Fig. 3 Conflictual chronostratigraphic datings of the Schrattenkalk Formation in the Helvetic domain based on microfossils (Bonvallet et al., 2019; Clavel et al., 2014; Schroeder et al., 2007), few ammonites (Bodin et al., 2006a; Föllmi and Gainon, 2008) and correlations based on sequence stratigraphic interpretations (Bodin et al., 2006a, b; Bonvallet et al., 2019; Godet et al., 2013)

the *T. vandenheckii* and the *G. sartousiana* zones. They attributed this bed to the maximum flooding surface (MFS) Ba3 of more or less comparable age. Based on a sequence stratigraphic interpretation of the Tierwis section, Bodin et al. (2006a) attributed the marlstone interval at the transition of the Drusberg Member to the Schrattenkalk Formation to the MFS Ba3, de facto attributing a maximal age for the installation of the Schrattenkalk platform in the Säntis area (Fig. 3). Nevertheless, the relationship between the Chopf Bed in distal platform environments and the facies change within the shallow-water urgonian succession remained unclear (Bonvallet et al., 2019). Clavel et al., (2014, p. 45) cast doubt on this hypothesis supported by two very poorly preserved Barremian ammonites figured by Bodin et al., (2006b, fig. 3E and F). Based on observations made in the French Subalpine chains (Haute-Savoie department), Clavel et al. (2014) suggest that the Schrattenkalk Formation arose during the earliest Barremian. Nevertheless, the use of a variety of tools as micro- and macro-fossils (e.g., Arnaud & Arnaud-Vanneau, 1991; Arnaud et al., 1998; Arnaud-Vanneau, 1980; Clavel et al., 1986, 2007, 2014; Frau et al., 2018a; Masse, 1976, 1995; Masse & Fenerci-Masse, 2008, 2017, 2018; Masse & Humbert, 1976; Masse et al., 2020) or sequence stratigraphic correlations and geochemistry (Bonvallet et al., 2019; Frau et al., 2018a, 2018b; Huck & Heimhofer, 2015; Huck et al., 2011, 2013; Wissler, 2001; Wissler et al., 2003) did not help to resolve all the existing conflicts of time correlation within the Schrattenkalk Formation.

3 Material and methods

The methods used for this study are essentially the same as described for the first part of the study of Pictet et al. (2022).

We carried out a sedimentological and palaeontological field study of the Schrattenkalk Formation based on sections in four reference areas (Tierwis-Grauchopf, Langtal-Säntis, Altmann and Litten-Chreialp—Tesel). The collected or reconsidered macrofossils are stored in the Naturmuseum St.Gallen (NMSG, ex-coll. Museum Heiden and Coll. Kürsteiner), in the inatura—Erlebnis Naturschau Dornbirn (Austria), in the Eidgenössische Technische Hochschule Zürich (ETHZ) and in the Musée cantonal de géologie of Lausanne (MGL, Coll. Föllmi).

Discontinuity surfaces are indicated on the lithological logs and figures and are numbered from D1 to D17. These surfaces were correlated with the sequence stratigraphic scheme of Arnaud (2005), derived from the Barremian stratotype of Angles (SE France). The sequence stratigraphic interpretation is given on the right side of the lithological logs. Sequence boundaries (SB) are indicated by red full lines, maximum flooding surfaces (MFS) by blue dot lines and transgressive surfaces (TS) by green dash-dot lines.

Geochemical measurements from the Tierwis-Grauchopf section were performed by Wissler (2001) and Bonvallet (2015). We used the carbon-isotope segments B1 to A1 (negative, stable or positive trend), that correspond to the nomenclature of Wissler, (2001) and Wissler et al., (2002, 2003) for the Barremian and lowermost Aptian stages.

The ammonite biozonation used in this work bases on the zonal scheme of the Tethys realm proposed at the 6th International Meeting of the IUGS Lower Cretaceous "Kilian Group" (Reboulet et al., 2018).

In order to avoid reproducing the profound nomenclatural confusion concerning the different carbonate units composing the Schrattenkalk Formation and affine units, the successive limestone units are named from bottom to top as S1 to S4-Gr. Each Schrattenkalk unit herein corresponds to an individual prograding platform body, which is characterised by its own petrographic and/or macrofaunal content. Schrattenkalk units are separated by flooding surfaces or flooding intervals such as the Rawil Member.

4 The key sections

The sections at Tierwis-Grauchopf, Langtal-Säntis, Altmann and Litten-Chreialp—Tesel are described following a northwest-southeast platform-to-basin transect.

4.1 The Tierwis-Grauchopf section

The Schrattenkalk Formation in the Tierwis area was described and/or logged by Heim (1905), Lienert (1965), Wissler (2001), Bonvallet (2015), Tajika et al (2017) and Bonvallet et al. (2019).

The transition from the Drusberg Member to the light-grey shallow-water carbonates of the Schrattenkalk Formation is progressive, occurring on a thickness of ca. 5 m. In this section, the neritic carbonate series of the latter only present the units S1 and S3 with from bottom to top:

1) A 100 m-thick cliff-forming unit S1 representing the 60% of the thickness of the whole formation. The cliff is massive, without marked stratification (Heim, 1905; Fig. 4A). Its base consists of a bioclastic facies and contains some oysters-bearing beds (Fig. 4B). The middle part is fairly coralliferous (Fig. 4C). Its top contains abundant rudist shells dominated by the Barremian rudists species *Agriopleura blumenbachi* (Studer, 1834) and *A. marticensis* (d'Orbigny, 1847) (Fig. 4D; see also Bollinger, 1988). The top of the Schrattenkalk unit S1 shows a very strongly karstified surface covered with a red palaeosol contain-

ing reworked pebbles and fragments of rudist shells (Fig. 4E; exposure surface E.s. on Fig. 5A);

2) A 25 m-thick *Orbitolina*-rich intercalation (Fig. 5A—Rawil Mb) of brownish, thin and well bedded limestones (Heim, 1905). This unit starts with a fossiliferous basal limestone containing abundant internal moulds of gastropods belonging to *Harpagodes pelagi* (Brongniart, 1821) and numerous rudist shells of Requieniidae like *Toucasia carinata* Matheron, 1842 and *Requienia ammonia* (Goldfuss, 1832). Above the basal limestone, brackish, grey marlstones and clayey-limestones (Fig. 5B) and shore deposits extremely rich in charophytes and tree trunks (Fig. 5C; Bonvallet et al., 2019) are deposited. Upwards, follows coral-bearing beds (Fig. 5D; see Baron-Szabo, 2021) grading upward into rudist-bearing beds, dominated by a requieniid-monopleurid assemblage. Near the top of the unit, a bioturbated firmground (D14) is observed (Fig. 5E). The surface is overlain by marlstones (Fig. 5A –O. l. bed) filling the bioturbations of the underlying firmground with a bioclastic sediment almost exclusively composed by the foraminifera *Palorbitolina lenticularis* (Blumenbach, 1805). Echinoids as *Pygaulus desmoulinsi* Agassiz, 1847 and *Heteraster oblongus* (Brongniart, 1821) are common (Figs. 5F and 6B);

3) A 25 m-thick Schrattenkalk unit S3 (Figs. 5A and 7A), which only represents 1/5 of the thickness of the formation. Unit S3 is well bedded (Heim, 1905) and very rich in rudist shells of Requieniidae (Fig. 7B). The terminal surface shows an irregular topography (Fig. 7A) of epikarstic appearance (Fig. 7C);

4) The irregular and corroded surface is covered by iron and phosphate crusts. The cavities are filled with an undated echinodermic limestone containing abundant phosphoclasts and pebbles of Schrattenkalk facies (Fig. 7C). The whole is capped by grey to brown glauconitic marlstones attributed to the Sellamatt Beds (Selun Member; Fig. 7A) of middle Albian age (Föllmi & Ouwehand, 1987).

Carbon and oxygen stable isotope measurements were performed in the Schrattenkalk Formation by Wissler (2001) (Fig. 8). The Schrattenkalk Formation was later resampled for higher resolution by Bonvallet (2015) and Bonvallet et al. (2019) who also measured the phosphorus content (Fig. 8).

The carbon stable-isotope record from the Schrattenkalk Formation in Tierwis-Grauchopf section exhibits five successive trends characterising the carbon isotope segments B3 to A1 following the nomenclature of Wissler (2001) but differing to his interpretation of the individual segments (in gray):

-Segment B3, first "stable" and then bearing decreasing values within the Drusberg Member and lowermost Schrattenkalk beds (refer to Pictet et al., 2022, fig. 5 for a more detailed curve of segments B1 to B3);—B4 with increasing values starting inside the lowermost Schrattenkalk beds and then stabilizing by around 2.7‰ and a top marked by a drop of 2‰ occurring just below the karstic surface D13;—B7 is characterized by a positive excursion to higher $\delta^{13}C$ values then stagnating by around 3.4‰;—B8 with a decreasing trend toward more negative values up to 2.8‰; A1 with increasing values up to 3.6‰. The lack of statistically significant correlation between $\delta^{13}C$ and $\delta^{18}O$ values (covariance $R^2 = 0.11$; Bonvallet, 2015, pp. 85 and 89) for the section of Tierwis-Grauchopf excludes a diagenetic modification of the primary carbonate C isotope signature.

The phosphorus (P) content shows three intervals inside the Schrattenkalk series with:—a general upward decrease trend across the unit S1, ending by strong fluctuations in the rudists-bearing beds;—increasing values in the overlying Rawil Member (Bonvallet et al., 2019; Stein et al., 2012a);—a new decrease in the unit S3;—a pronounced peak starting a little below the terminal karstified surface of the Schrattenkalk, due to karstic infiltrations from the overlying Garschella Formation (Bonvallet et al., 2019).

4.2 The Langtal-Säntis section

Like in the Tierwis-Grauchopf section, the uppermost beds of the Drusberg Member still contain ammonites from the *T. vandenheckii* Zone (Fig. 9B; Pictet et al., 2022). These beds seem to extend stratigraphically further upward than in the Tierwis-Grauchopf section before they pass progressively, over a distance of approx. 5 m, into the Schrattenkalk unit S1 (Fig. 9C). At Langtal-Säntis, the unit S1 is only about 10 m-thick, in contrast to a thickness of 100 m in Tierwis-Grauchopf. The unit S1 ends with a noticeable discontinuity surface D12 (Fig. 9D). Above this surface, the Schrattenkalk unit S2 starts with thin-bedded bioclastic and oolitic

(See figure on next page.)

Fig. 4 **A** Overview of the Tierwis-Grauchopf section of the lower part of the Schrattenkalk Formation from the car cable. The lowermost unit S1 overlains the Drusberg Member (Tierwis Formation) and is topped by the Rawil Member. **B** Focus on the oysters-bearing bioclastic facies from the base of the cliff of unit S1. **C** Focus on the coralliferous facies of the middle interval of unit S1. **D** Focus on the *Agriopleura*-bearing beds the upper part of unit S1. **E** Focus on the strongly karstified surface at the top of unit S1. The epikarst is covered by a red palaeosol bearing many reworked pebbles and fragments of rudist shells

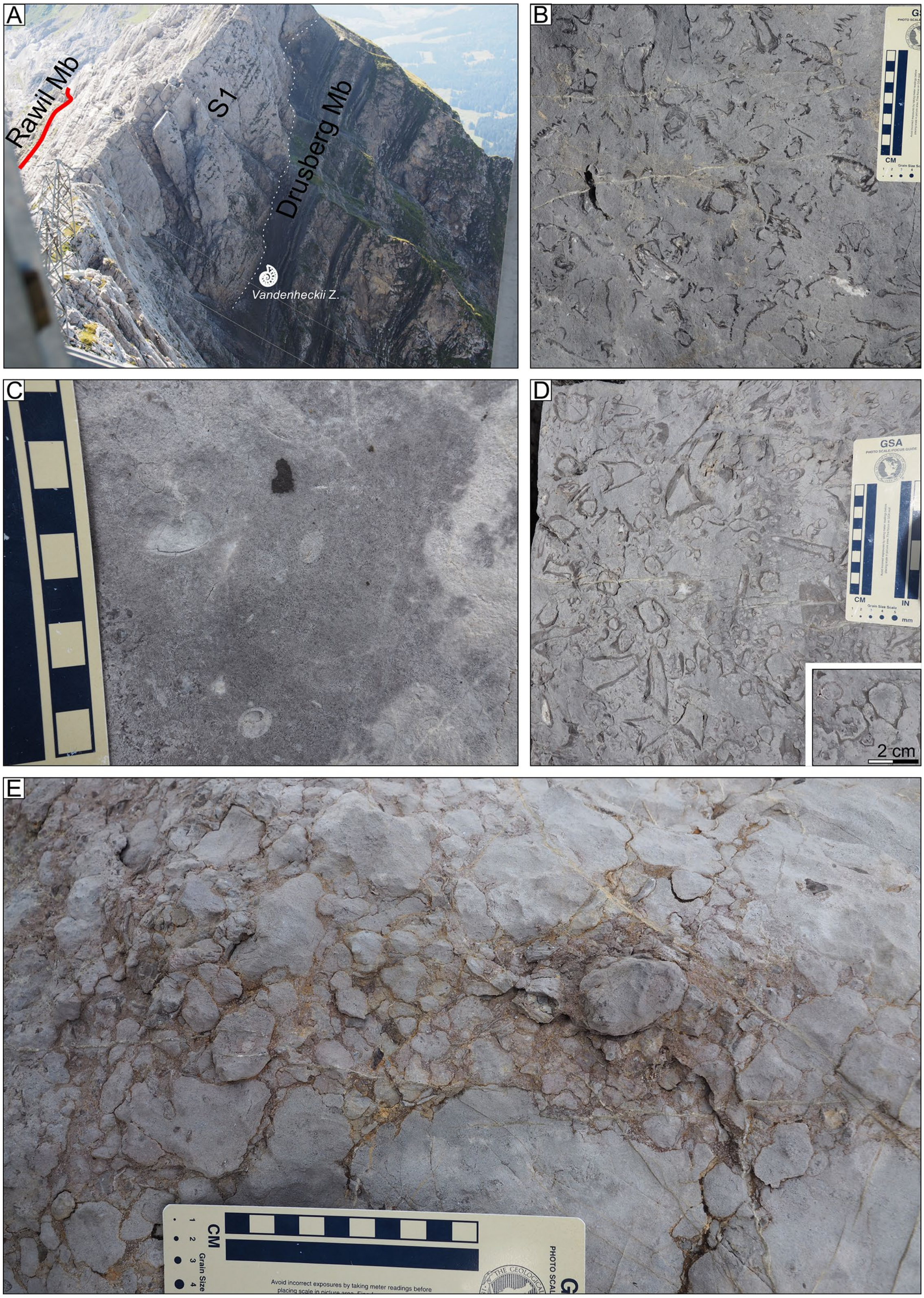

Fig. 4 (See legend on previous page.)

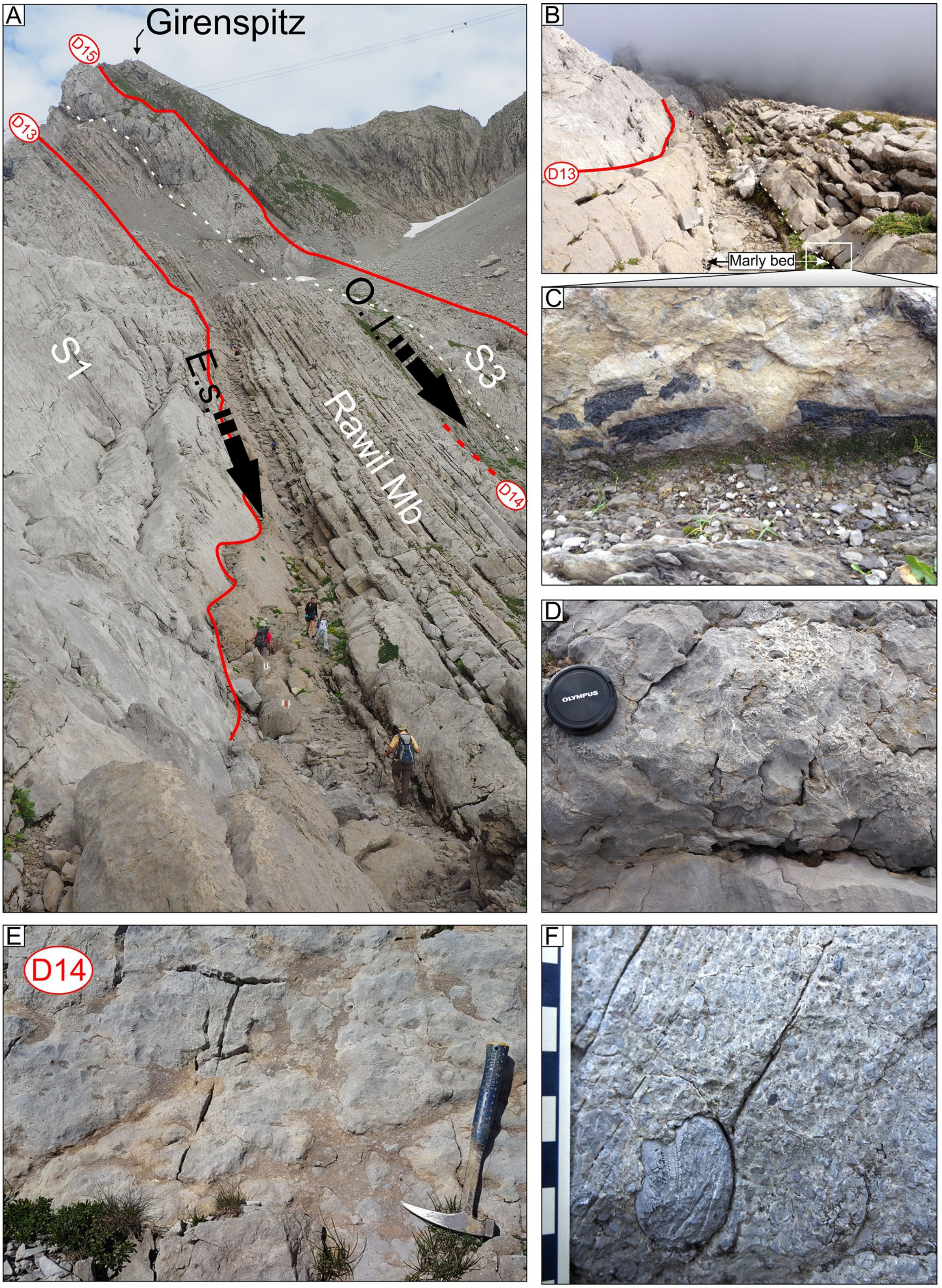

Fig. 5 **A** Overview of the Tierwis-Grauchopf section of unit S1, the Rawil Member and of unit S3. E.s. = exposure surface. O.I. = *Orbitolina*-bearing level. **B** Focus on the lower marly intercalation of the Rawil Member. **C** Focus on the tree trunks (ca. 50 cm long) at the top of the lower marly intercalation. **D** Focus on the coral carpets above the lower marly intercalations. **E** Focus on the firmground at the base of the upper marly intercalations. **F** Focus on the *Orbitolina*-rich rudstone of the upper marly intercalation associated to *Heteraster oblongus* (Brongniart, 1821)

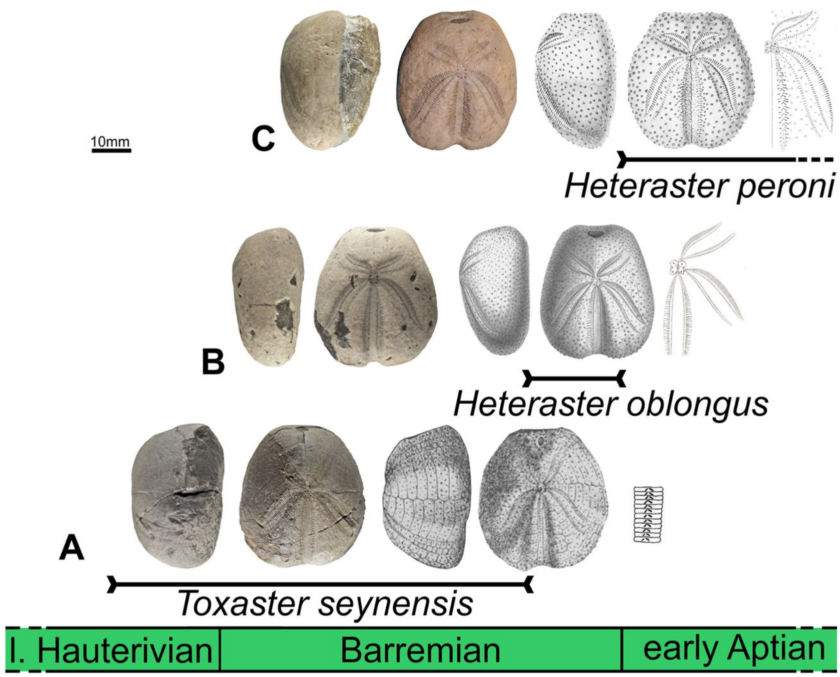

Fig. 6 Echinoids of biostratigraphical value present in the uppermost Hauterivian to lower Aptian series (Tierwis Formation, Schratenkalk Formation and Garschella Formation pro parte) of the Alpstein massif. **A** *Toxaster seynensis* (Lambert, 1920), drawing by Lambert (1920) and organization of the pores of the odd ambulacrum according to Clavel in Charollais et al. (2009). **B** *Heteraster oblongus* (Brongniart, 1821), drawing by d'Orbigny (1853–1855). **C** *Heteraster peroni* (Ficheur, 1900), drawing by Ficheur (1900)

series before grading into a massive limestone cliff with a thickness of about a 100 m. The unit S2 is overlain by the Rawil Member and the Schrattenkalk unit S3 (Fig. 9B).

4.3 The Altmann section

The Schrattenkalk Formation progressively arises from the Drusberg Member, representing the *G. sartousiana* Subzone (Pictet et al., 2022). The Schrattenkalk unit S1 and its type fauna is missing here as, according to the ammonites, it sedimented under the Drusberg facies. Therefore, the Schrattenkalk cliff presents the successive units S2 to S4-Gr with from bottom to top:

1) A 116 m-thick massive unit S2 starting with 20 m of obliquely stratified limestones (Fig. 10A–C). A juvenile specimen of Barremitidae related to the genus *Barremites* or *Montanesiceras* was found in the scree by Christian Klug (Paläontologisches Institut und Museum Zürich; Fig. 11A). A fragment of a large ammonite was found in the lower third of the unit S2 by T. Kempf (Lienert, 1965, p. 22). Lienert reported this fragment to a possible "precursor" to the "Parahoplitidae" found in the "Upper" Schrattenkalk of Brunnen (Canton of Schwytz). The specimen was unfortunately not found in the collections of the Swiss Federal Institute of Technology Zurich (ETHZ) and so probably never collected.
2) A 20 m-thick interval with two tender bundles, corresponding to the Rawil Member (Fig. 10C).
3) A 28 m-thick, better stratified limestone unit S3 (Figs. 10C).
4) A 3 m-thick, stratified limestone unit S4-Gr richer in echinoid debris and presenting glauconite grains (Fig. 10C and D), indicating a transition to the overlying Garschella Formation.

Geochemical analyses of the stable carbon and oxygen isotopes were performed by Wissler (2001, p. 109) but the sample spacing is too loose for supporting any interpretation.

4.4 The Litten-Chreialp—Tesel section

The Schrattenkalk Formation was never really studied in detail in this part of the Alpstein massif.

Our observations were made along the anticline, mostly in Litten-Chreialp section situated on the eastern side of the Tristen Sattel (Coordinates 2′745′7347;1′232′270 system CH1903+/LV95) and along the path from Eggsteihalde (coord.: 2′745′347;1′231′654) to Chridegass (coord.: 2′645′318;1′231′981).

The Drusberg Member, outcropping well in Litten-Cheialp, progressively passes upward to the Schrattenkalk series, which present the successive units S2 to S4-Gr with from bottom to top (Fig. 12A):

1) A 100 m-thick limestone unit S2, presenting an alternance of beds, dominated by bioclastic facies, grading to a massive cliff (Fig. 12B, D and E). The base of the unit S2 yielded the echinoid *Pygaulus desmoulinsi* Agassiz, 1847, while the upper and massive part contains abundant rudist shells belonging to *Agriopleura marticensis* (d'Orbigny, 1847) (Fig. 12C) and the gastropod *Harpagodes pelagi* (Brongniart, 1821);

In the Tesel section, along the path (Figs. 12D and E), the Schrattenkalk Formation is very steeply inclined to slightly overturned (Fig. 13). It continues with:

2) An about 4 m-thick Rawil Member with a tender interval composed of thin-bedded clayey limestones grading upward to white massive carbonates;
3) A 30 m-thick Schrattenkalk unit S3 (Fig. 12D and E), in which the rudist fauna consist only of representatives of the family Requieniidae. The top surface looks like a discrete bioturbated firmground;
4) A 17 m-thick unit S4-Gr (Figs. 12D–E and 13C–D) made of fine, light grey to grey and weakly glauconitic echinodermic limestones. The base is composed of a 2 m-thick bioclastic limestone, presenting a cross-stratification. Its top surface shows a discrete bioturbated firmground. This surface is overlain by a more marly and strongly bioturbated 1.5 m-thick intercalation. This marlstone is rich in orbitolinids, such as *Palorbitolina lenticularis* (Blumenbach, 1805) (Fig. 12F), in echinoids such as *Heteraster peroni* Ficheur, 1900 (Fig. 6C) and contains abundant small-sized rudist shells of Requieniidae. The unit ends by a well-visible firmground D16 injected with a quartz sand.

This uppermost discontinuity surface marks a strong sedimentological change toward more friable and dark-coloured series which are attributed to the “middle” Cretaceous Garschella Formation.

5) A 9 m-thick grey and coarse-grained echinodermic limestone of the uppermost Aptian Brisi Member (Figs. 12D–E and 13D).

4.5 South-eastern mountain range, close to the Rhine valley (Stauberen-Hoher Kasten-Kamor)

In this range, the Schrattenkalk series is represented by a single limestone cliff (Fig. 14B).

The Schrattenkalk and Garschella formations were mostly observed along the road from Rüthi to the Kamor (Schlatt-Mätzenacker, Fig. 14A, coord.: 2′759′093;1′241′164 to 2′758′902;1′241′083).

The sedimentary succession measures around 140 m-thick and is represented by the units S3 and the Grünten Member with, from bottom to top:

1) The lower two thirds of the unit S3 are composed of bioclastic, mostly echinodermic cross-stratified limestones (Figs. 14A, D and E). In the upper third of the unit, these bioclastic limestones grade into rudist-bearing beds dominated by the Requienidae, a typical assemblage of the unit S3. The unit ends by a corrugated and bored hardground (D15; Figs. 14F and G).
2) The surface of the unit S3 is overlain by the Grünten Member (Garschella Formation). It is much coarser-grained echinodermic grainstones, associated to glauconite, orbitolinids (Fig. 14H) and large corals (e.g., in Bergli section). The unit ends with a corrugated firmground D16.
3) A 1 m-thick marly-limestone with corals grading upward to a very fractured, coarse-grained echinodermic limestone of the Brisi Member.

5 Discussion

5.1 Onset and development of the Schrattenkalk platform in the Alpstein massif

The successive thrust sheets composing the Alpstein massif of the Helvetic Säntis nappe are most likely inherited from tilted blocks as discussed in Zerlauth et al. (2014) and Pictet et al. (2022). As in the case of the Tierwis Formation (Bodin et al., 2006b; Pictet et al., 2022), synsedimentary tectonics most likely had an impact on the development and spatial distribution of the different carbonate bodies forming the Schrattenkalk platform.

5.1.1 Tilted block of Tierwis-Grauchopf

Based on carbon-stable isotopes analyses (Fig. 8) and their correlations with the basinal record (see also Wissler et al., 2002), Wissler (2001) attributed the onset of the Schrattenkalk platform at the Tierwis-Grauchopf section to the upper part of the B3 geochemical segment which he correlated with the late *T. vandenheckii* Zone. Above, Wissler attributed the Schrattenkalk unit S1 to

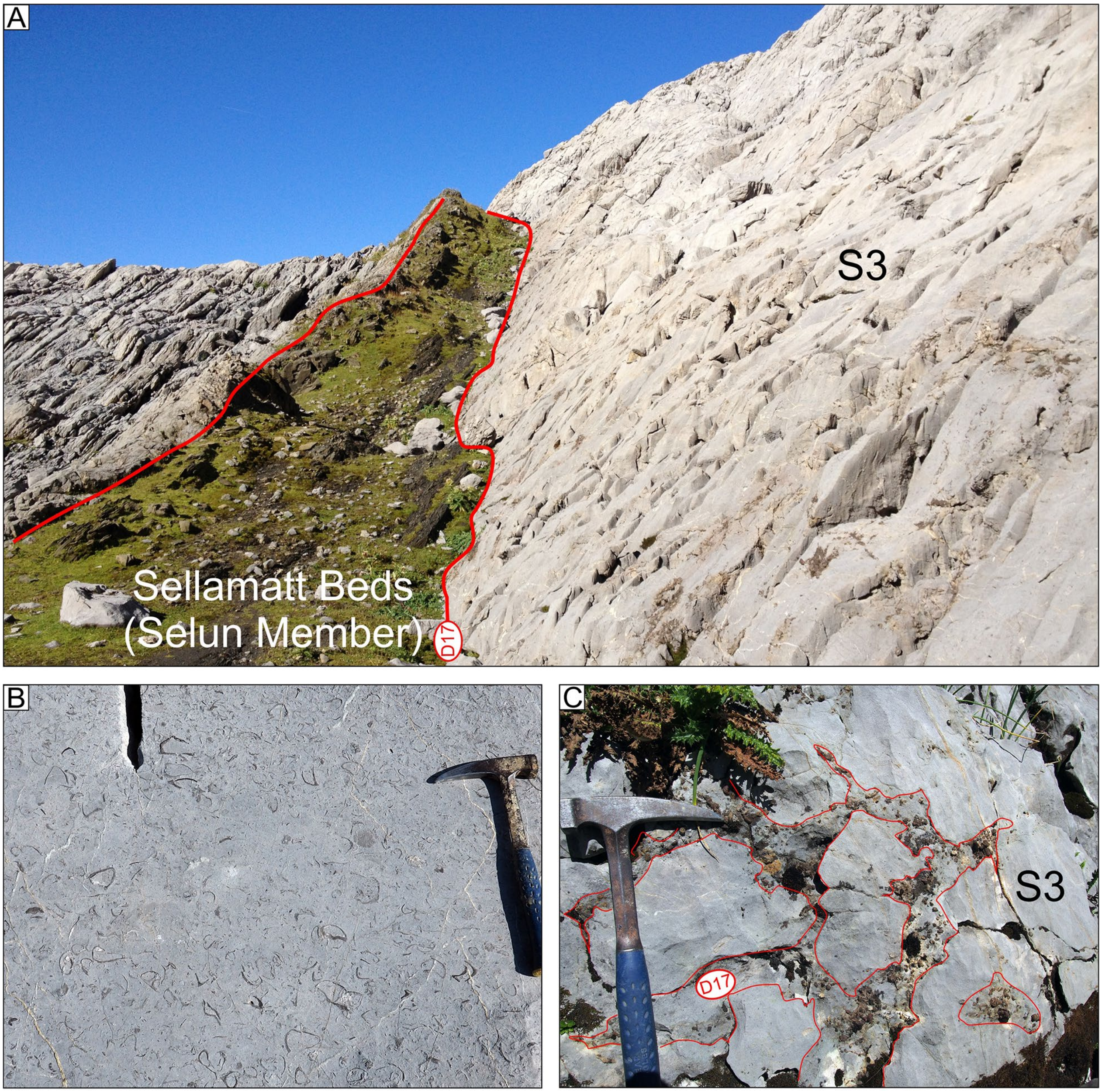

Fig. 7 **A** Overview in the Tierwis-Grauchopf section of the top of the Schrattenkalk Formation (unit S3) overlain by the Garschella Formation represented here by the Selun member. **B** View of the Requienidae-bearing beds of unit S3. **C** Focus on the irregular topography with epikarstic features on top of unit S3, filled with a phosphatic conglomerate

the uppermost B3, B4 and B5 geochemical segments, which he correlated with the late *T. vandenheckii* Zone and the *G. sartousiana* Zone. Nevertheless, we notice that Wissler et al. (2003) situate the segments B4 and B5 below the Chopf Bed in the Alvier section, a bed dated by ammonites in Bodin et al. (2006a) from the transition between the *T. vandenheckii* and the *G. sartousiana* zones. Thus, the segments B4 and B5 belong to the *T. vandenheckii* Zone. The Rawil Member and the Schrattenkalk unit S3 were attributed to the isotopic segments B6 to A2 and correlated with the *I. giraudi* to *D. forbesi* zones. At the opposite, on the basis of the orbitolinids foraminifers and sequence stratigraphic interpretations, Bonvallet et al. (2019) correlated our Schrattenkalk unit S1 with the *T. vandenheckii* to *M. sarasini* zones, while the Rawil and the "upper" Schrattenkalk unit were

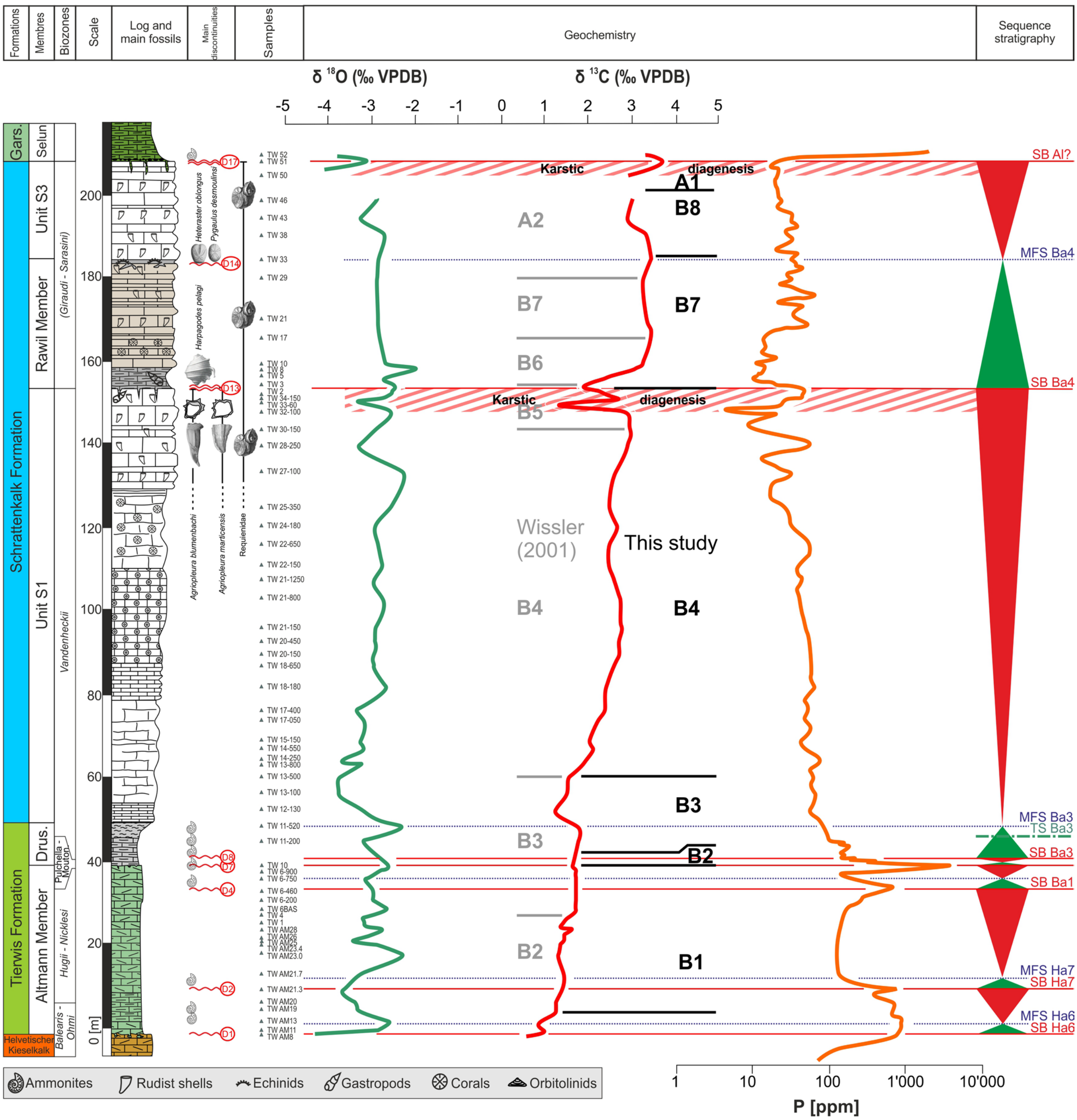

Fig. 8 Tierwis-Grauchopf section. Lithological log modified after Wissler (2001) with main fossil-bearing levels and stratigraphical extension of rudist species/families, discontinuity surfaces (D1 to D17), geochemical analyses and sequence stratigraphic interpretations. Samples' positions are form Bodin et al. (2006b), Bonvallet (2015), Bonvallet et al. (2019) and Godet et al. (2013) and correspond to the phosphorus (orange line) curve from Bonvallet et al. (2019). The carbon and oxygen isotope curves (red and green lines) are form Wissler (2001). Isotopic segments B1 to A2 reported on the δ13C curve are labelled after the nomenclature of Wissler (2001), and Wissler et al., (2002, 2003). Rudist-shells drawings from Matheron (1842) and from Pictet and Campiches (1868–1871). Rudist-cross sections modified after Masse and Fernerci-Masse (2015). *Harpagodes* drawing from Pictet and Renevier (1854–1858). Echinoids drawings from Pictet and Renevier (1858)

correlated with the lower Aptian series. For our part, we date the units S1 to S4-Gr using macrofossils assemblages, containing ammonites, rudists, echinoids and gastropods.

The ammonite sampling in the upper Drusberg series of the Tierwis-Grauchopf section indicates the *T. vandenheckii* Zone (Pictet et al., 2022), which is in accordance with Wissler, (2001). Based on very tenuous

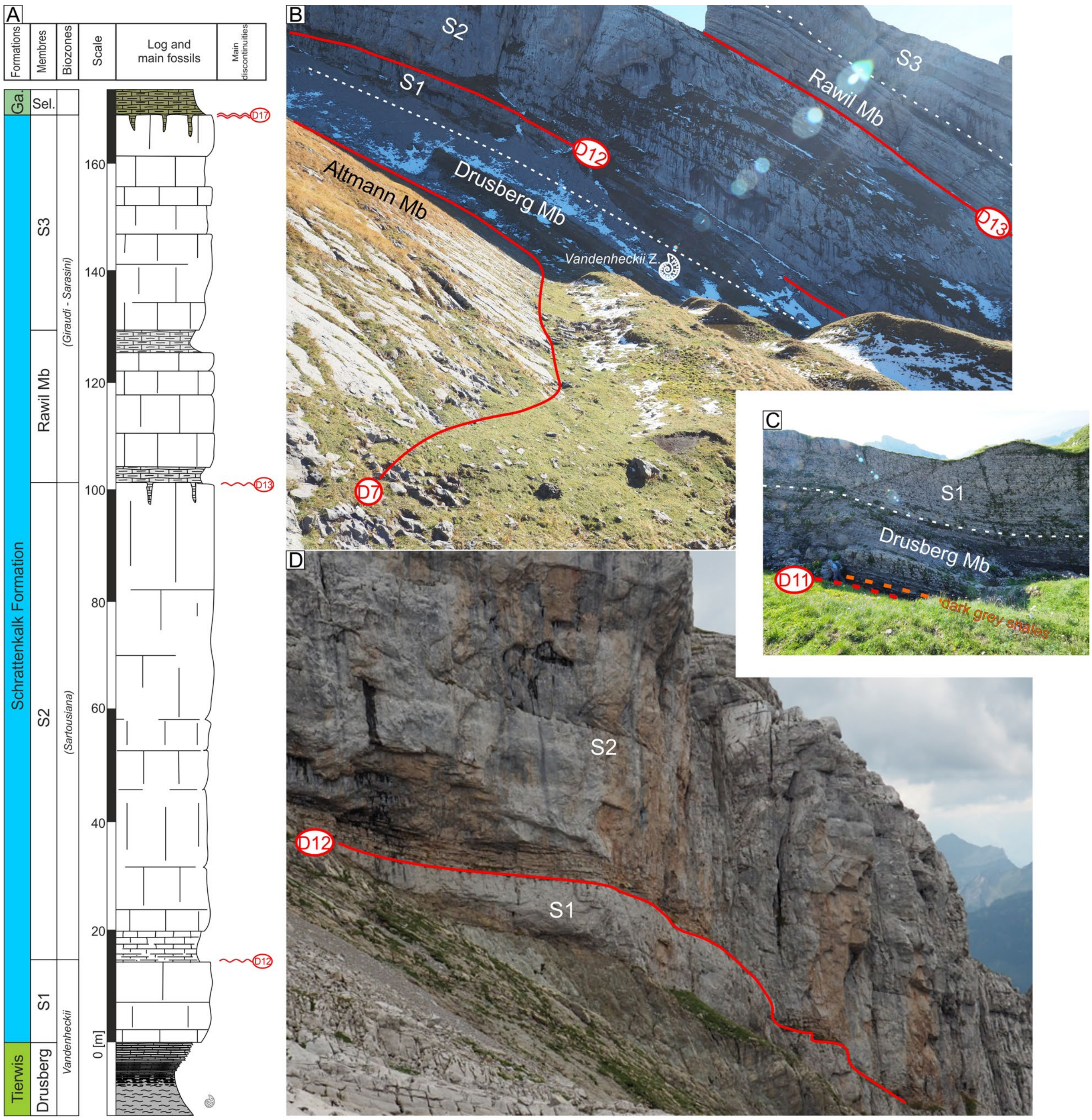

Fig. 9 **A** Langtal-Säntis section. Lithological log with discontinuity surfaces (D12 to D17). **B** Overview of the section looking north eastward. **C** Focus on the Drusberg-Schrattenkalk transition at Langtal. **D** Focus on the boundary between units S1 and S2 characterised by thin-bedded bioclastic limestones, which form the base of unit S2

observations made on thin sections, Bonvallet, (2015) and Bonvallet et al. (2019) suggested the presence of a major discontinuity surface with meteoric characters at the top of the Drusberg Member. Our field observations show a progressive onset of the Schrattenkalk Formation which rises from the Drusberg Member without any sedimentary interruption. Bonvallet, (2015) and Bonvallet et al. (2019) attributed their exposure surface to the important regressive marine phase close to the boundary between the early and late Barremian. This regression would have led to the emersion of the hemipelagic sediments in the proximal part of the slope and to the deposition of a lowstand systems tract in distal slope. However, the ammonites sampling in the Tierwis section allows to locate the boundary between the early and late Barremian 21 m below the base of the Schrattenkalk

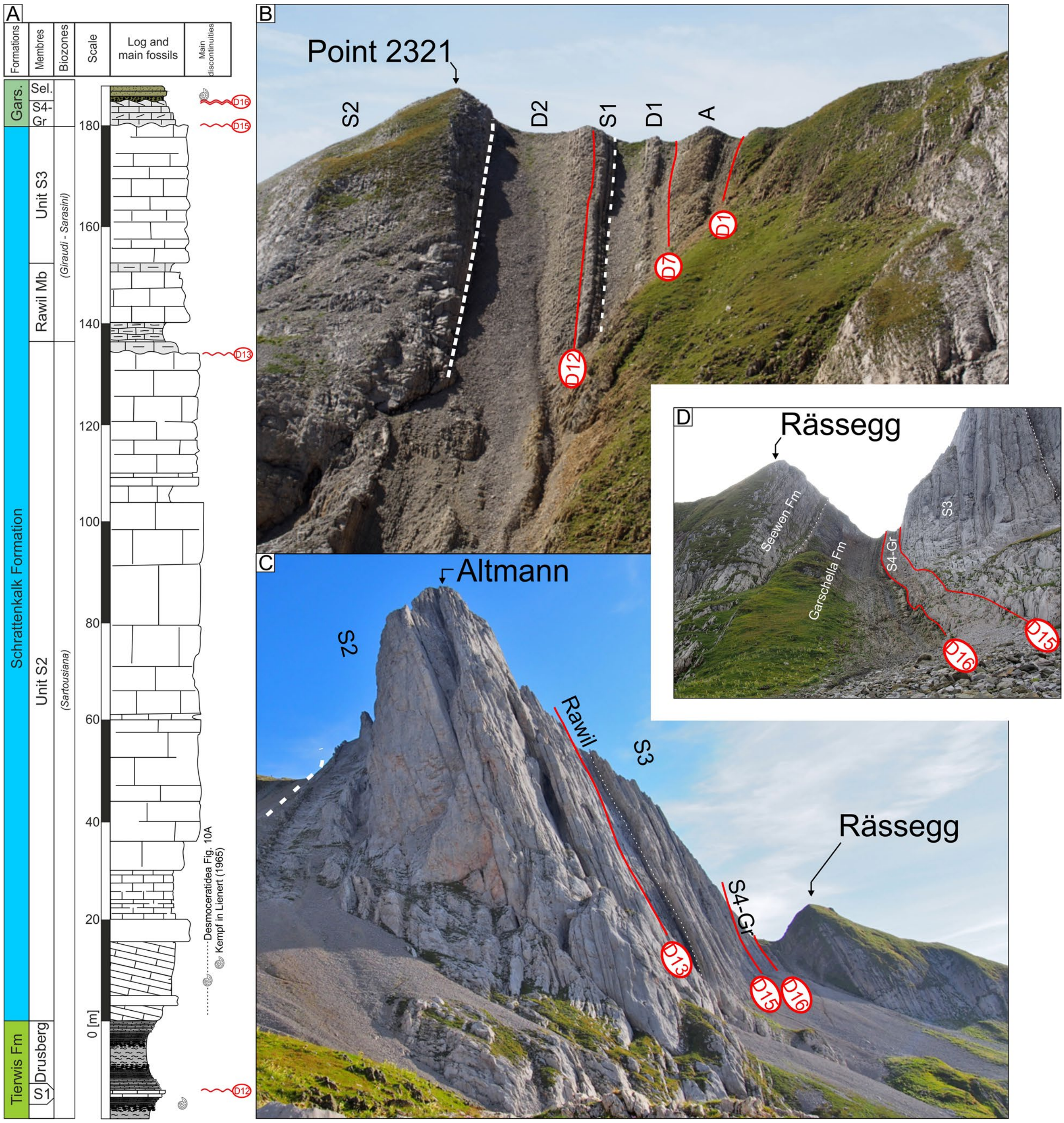

Fig. 10 **A** Altmann section. Lithological log modified after Wissler (2001) with discontinuity surfaces (D1 to D16). **B** Overview of the section in the face of our Altmann section, looking south westward. **C** Overview of the Altmann section looking north eastward. **D** Focus on the uppermost levels of unit S3, the unit S4-Gr and the overlying Garschella and the Seewen formations

Formation, at the first firmground surface (firmground 1 in Pictet et al., 2022, fig. 5). We assume that the overlying thick limestone dominated-unit forming the base of the Dursberg Member could represent the lowstand systems tract deposits of the sequence B3 whose age is indicated by the presence of *Toxancyloceras* sp. (see Pictet et al., 2022, p. 21).

The occurrence of the Barremian rudist genus *Agriopleura* Kühn, 1932 in the uppermost metres of the Schrattenkalk unit S1 is in accordance with an age not younger than the *G. provincialis* Subzone, since the last occurrence datum of the genus *Agriopleura* in the western Tethys is situated at the top of this subzone (Léonide et al., 2008, 2012; Masse & Fenerci-Masse, 2011; Masse

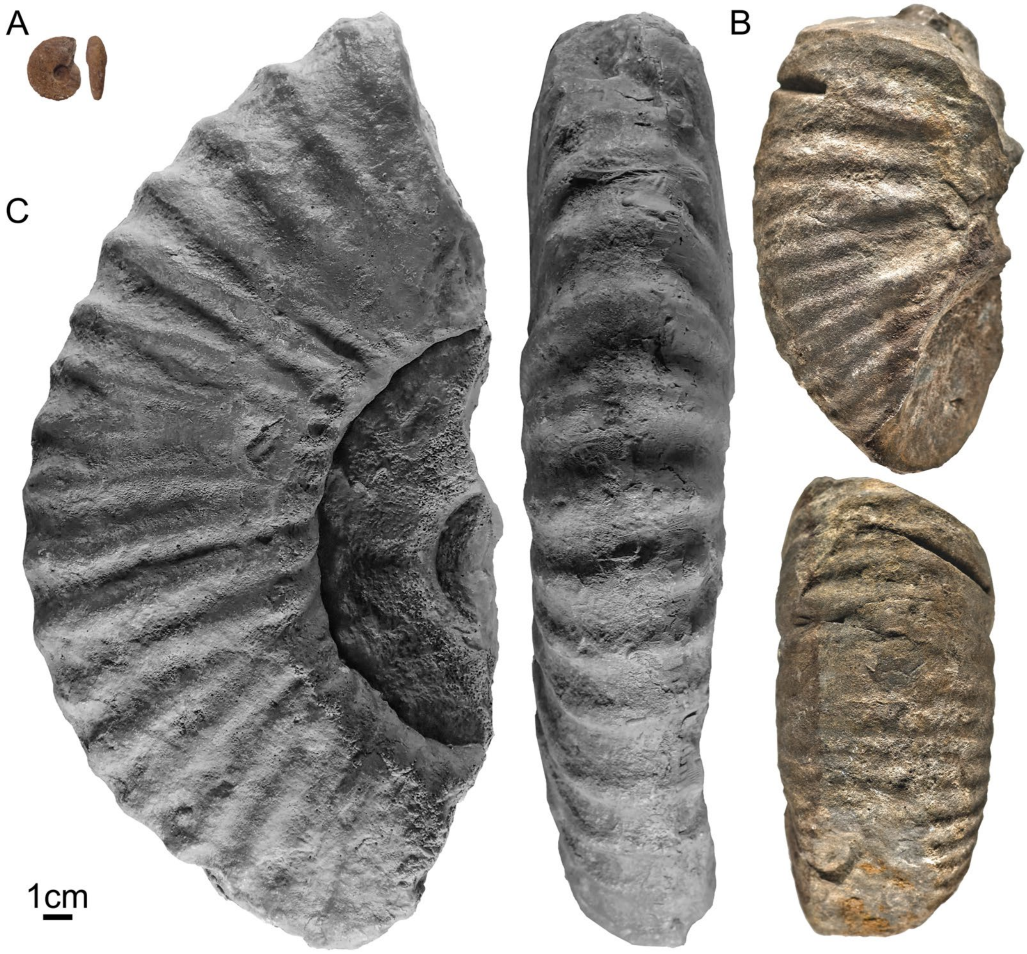

Fig. 11 Rare ammonites of the Schrattenkalk Formation (**A** and **B**) and from the distal slope equivalents (**C**). **A** Silicified Barremitidae collected ex-situ but judged to come from the lower quarter of unit S2, Naturmuseum St.Gallen, cat. no. Coll. PK.6A.36.02, Altmann section **B** *Kutatissites* sp., Altmann section, Naturmuseum St.Gallen, ex-coll. Museum Heiden, cat. no. STG.13 F-5672.2, stratigraphic level of sampling unknown **C** *Martelites martelli* Conte, 1989 coming from Brau near Bezau, Austria, Inatura Museum of Dornbirn, cat. no. P. 26123, photograph of the plaster cast, stratigraphic level of sampling unknown

et al., 2020). The co-occurrence of the species *Agriopleura blumenbachi* (Studer, 1834) helps to restrict this dating to the *T. vandenheckii* Zone (Masse & Fenerci-Masse, 2015; Masse et al., 2020). The paleontological dating differs slightly from the geochemical attribution of Wissler (2001) for the Tierwis-Grauchopf type section by excluding the *G. sarousiana* Zone. The transition between the Schrattenkalk unit S1 and the Rawil Member shows a very strongly karstified surface covered with a red paleosol containing reworked pebbles and fossils. The layer is passing upward into a brackish facies and into shore deposits extremely rich in charophytes and tree trunks. The Rawil Member and the overlying Schrattenkalk limestones contain a rudist fauna composed exclusively by species of the Family Requienidae (mostly *Toucasia* and *Requienia* spp.). The Rawil Member and the Schrattenkalk unit S2 are dated in the literature as early Aptian (e.g., Bollinger, 1988; Bonvallet et al., 2019; Lienert, 1965; Renevier, 1877, 1881, 1890; Schenk, 1992; Stein et al., 2012a), an age attribution that will be discussed later. At this point of the discussion, the rudist assemblage is not in contradiction with this lower Aptian age. Following these facts, a long-lasting exposure event is inferred, corresponding to our Schrattenkalk unit S2. By the way, this long exposure event of the proximal platform could be explained by the tectonic movements of the block of Tierwis-Grauchopf.

5.1.2 Tilted block of Langtal–Säntis

The series of the Tierwis Formation are very similar to those of the Tierwis section. On the other hand, the Schrattenkalk Formation is markedly different. The

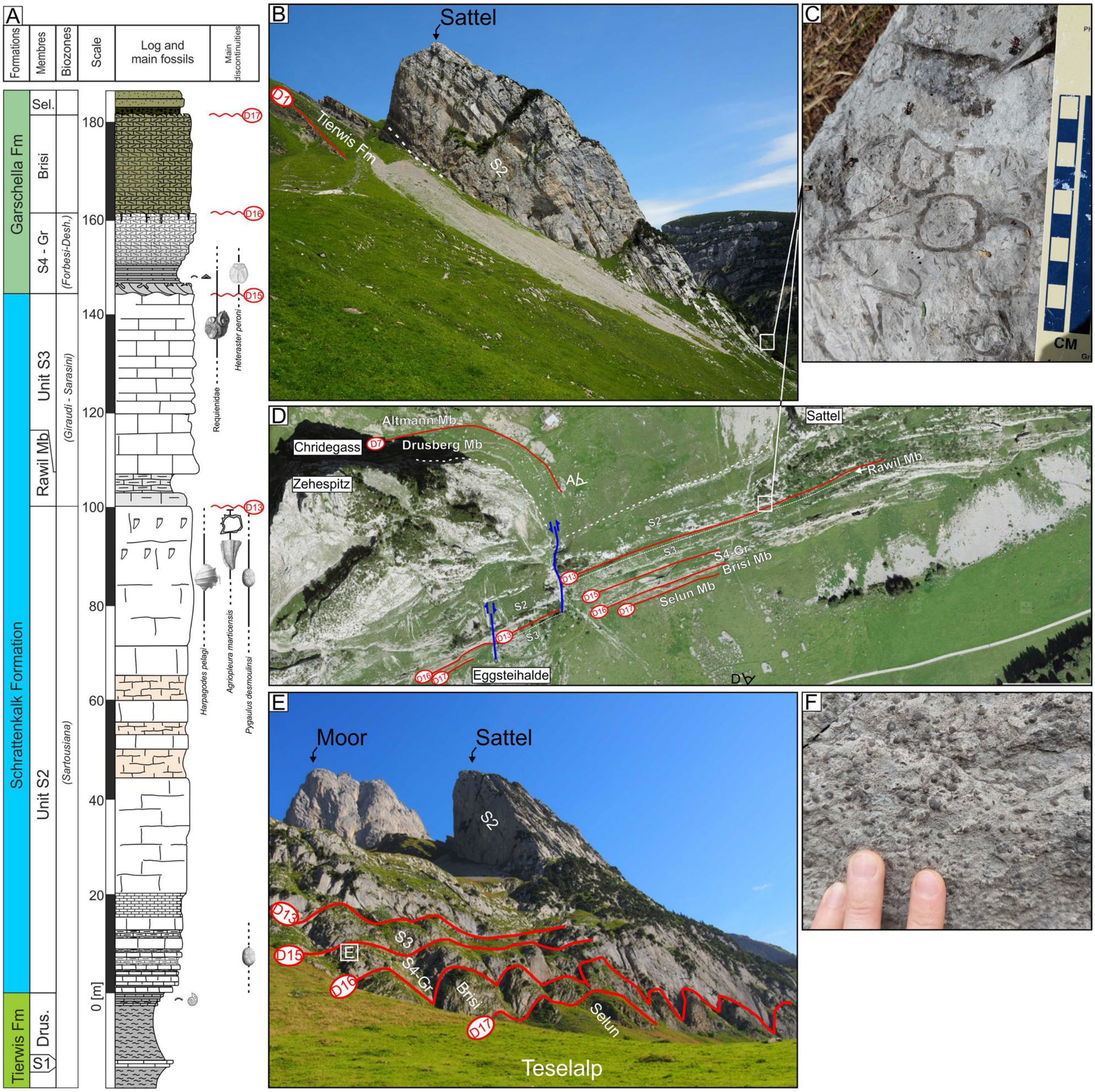

Fig. 12 **A** Lithological log of Litten-Chreialp-Tesel section with discontinuity surfaces (D13 to D17). Rudist-shells drawings from Matheron (1842) and from Pictet and Campiches (1868–1871). Rudist-cross sections modified after Masse and Fernerci-Masse (2015). *Harpagodes* drawing from Pictet and Renevier (1854–1858). Echinoids drawings from Pictet and Renevier (1858) and Lambert (1920). **B** Litten-Chreialp—Tesel section. North-eastward view of Sattel from the pastures below Chridegass allowing the observation of the Tierwis Formation and lower part of the Schrattenkalk Formation (unit S2). **C** Focus on the *Agriopleura*-bearing beds on top of unit S2. **D** Orthophoto (© swisstopo) between Zehespitz and Sattel with the path rising from Eggsteihalde to Wildhuser Schofbode on which are reported the main lithostratigraphic units and discontinuity surfaces are displayed. **E** North eastward view of Sattel from the lower pastures of Tesel showing the lithostratigraphic succession and the discontinuity surfaces between the unit S2 of the Schrattenkalk formation and the Selun Member of the Garschella Formation above. **F** Focus on the Palorbitolina lenticularis-bearing marlstone in the lower third of the Grünten Member cropping out along the path

Schrattenkalk unit S1 is only about 10 m-thick, ending by a noticeable discontinuity surface D12 (Fig. 9). Above this surface, a thick and massive Schrattenkalk unit S2 is present (Fig. 9) followed by the Rawil Member and the Schrattenkalk unit S3 which are also thick.

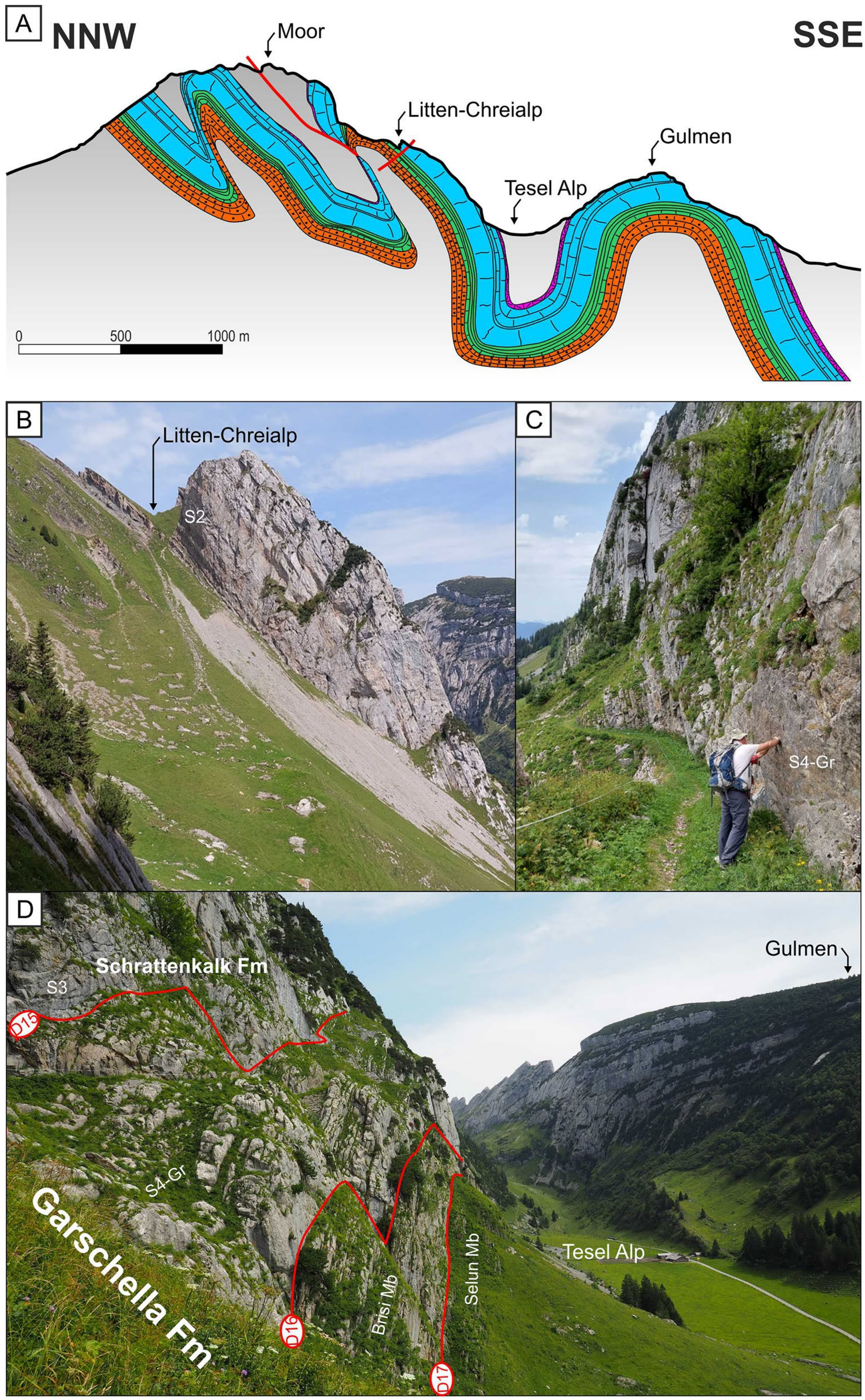

Fig. 13 **A** Geological cross-section between Moor and Gulmen modified after Kempf (1966). The colours refer to Fig. 1. **B** North eastward view on the Litten-Chreialp section from Chridegass. **C** South-westward view on the slightly overturned fold along the path from Eggsteihalde to Wildhuser Schofbode where the Grünten Member is easily accessible. **D** North eastward view on the Garschella Formation, from the same path

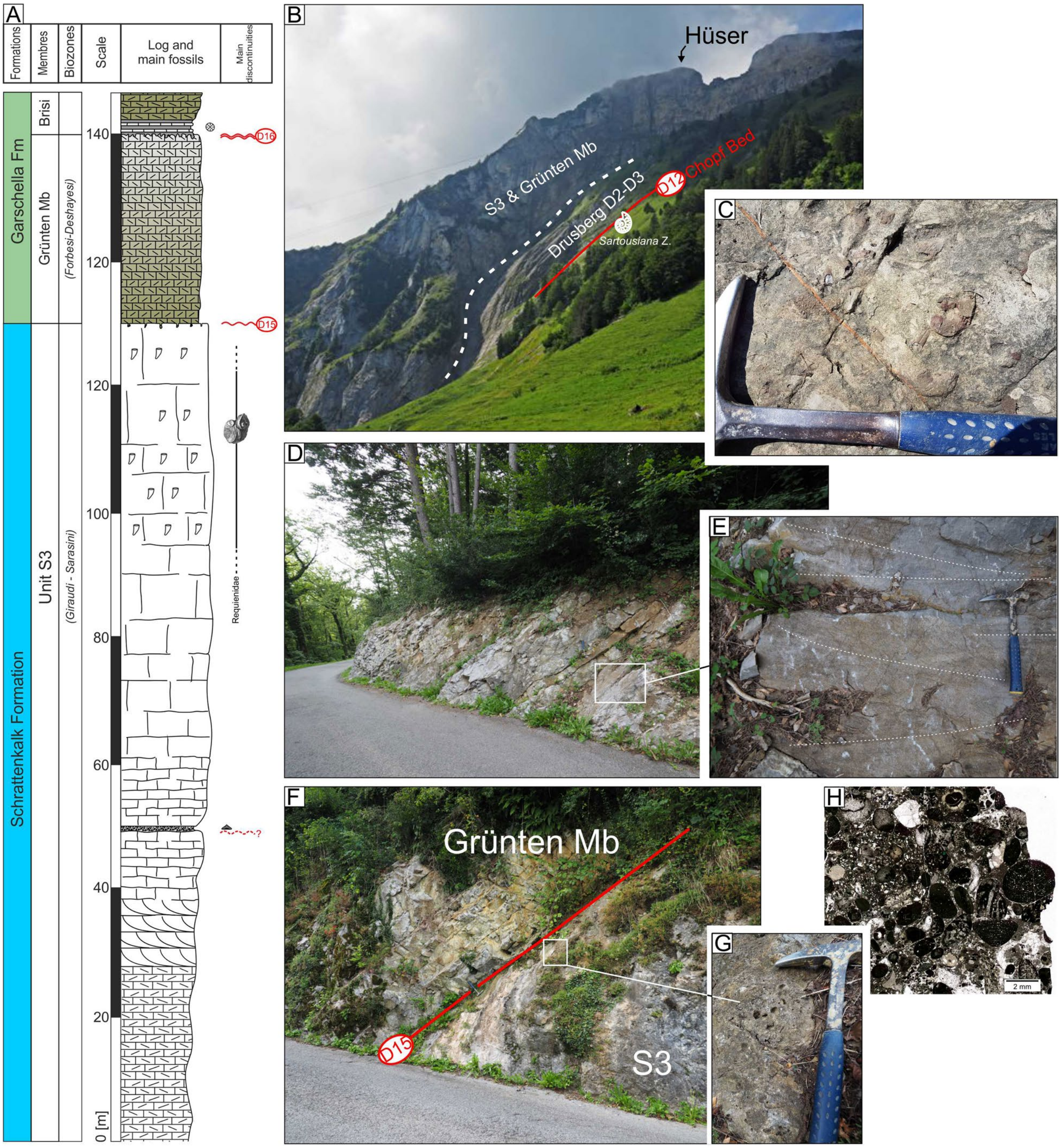

Fig. 14 **A** Lithological log of Mätzenacker section with discontinuity surfaces (D15 and D16). Rudist-shell drawing from Matheron (1842). **B** South westward view from Vorderalp (Frümsner Alp) on the Hüser cliff along the south eastern anticline. The succession is composed of marlstones of the upper part of Drusberg Member (D2; Tierwis Formation pro parte) transforming into a succession of carbonates of the Schrattenkalk Formation and the Grünten Member (Garschella Formation pro parte). **C** Focus on the glauconitic Chopf Bed and its phosphatic ammonites in Alp Wis. **D** View of the irregularly bedded, bioclastic, mostly echinodermic limestones (unit S2?–S3) along the Brunnenberg road at Mätzenacker. **E** Focus on the cross-stratification inside the echinodermic limestones. **F** Contact between the Schrattenkalk unit S3 and the Grünten Member along the Brunnenberg road at Mätzenacker. **G** Focus on the bored firmground surface D14. **H** Thin section in the bioclastic limestone of the Grünten Member, characterized by its glauconite gains and abundant orbitolinids, Bergli section

5.1.3 Tilted block of Altmann, Tesel and Frümsner Alp

The Drusberg Member differs from the situation in the previous blocks. The Drusberg Member is thicker and stratigraphically extending upward at least up to the *G. sarstousiana* Subzone according to the ammonite data (Pictet et al., 2022). Beds corresponding to the Schrattenkalk unit S1 from the previous and more internal sections are here represented by a 2 m-thick succession of light grey, hard limestones beds, intercalated in the middle of the Drusberg Member (Fig. 10B). This limestone bundle locally shows some bioclastic flows constituted of neritic material remobilised from the carbonate platform. The echinoid *Pygaulus desmoulinsi* Agassiz, 1847, collected in the basal beds of the unit S2, and the presence of *Harpagodes pelagi* (Brongniart, 1821) in the upper beds, indicates that this unit is not older that the *G. sartousiana* Zone (see discussion in Pictet, 2021). The presence of the rudist genus *Agriopleura* in the upper beds indicates that the unit S2 cannot be younger than the *G. provincialis* Subzone but not older either, as the species *Agriopleura blumenbachi* (Studer, 1834) is no longer present. Thus, the faunal association of the unit S2 corresponds to the *G. sartousiana* and *G. provincialis* subzones (according to the biostratigraphy of *Agriopleura* species; Masse & Fenerci-Masse, 2015; Masse et al., 2020).

An interesting fragment of ammonite labelled “Altmann” is stored in the Naturmuseum St.Gallen. This fragment belongs to the genus *Kutatissites* (Fig. 11B). Unfortunately, the original layer of the find is not indicated on the label. The fragment has a grey matrix that resembles the Drusberg facies and devoid of glauconite grains. This genus is restricted to the latest Barremian *M. sarasini* Zone and earliest Aptian *D. oglanlensis* Zone (see Frau et al., 2018a). This age is incompatible with the faunas known from the Drusberg Member and the Schrattenkalk unit S2. As a result, it is extremely unlikely that this ammonite comes from the Drusberg Member. On the other hand, the Rawil Member in this more distal setting of the platform area begins to show some clayey limestone beds, from which this specimen could have its origin.

In this south eastward situated part of the transect, the unit S4-Gr appears for the first time with a thickness of only a few metres and visually hardly differs from the Schrattenkalk unit S3 below. The echinodermic and slightly glauconitic limestone is nearly devoid of any rudist shells, and therefore should correspond to the “Schrattenkalk—Echinodermic breccia” of Heim (1905) and to the “glauconitischer Schrattenkalk (Grüntenschichten)” of Heim and Baumberger (1933, p. 212). In the Tesel section, this sedimentary unit starts to differ more clearly from the underlying Schrattenkalk unit S3 by its thin-bedded limestone beds and by the appearance of a *Palorbitolina*-rich marly level in its lower third. However, it also contains small-sized rudist shells of *Toucasia* Munier-Chalmas, 1873. The discovery of the echinoid *Heteraster peroni* Ficheur, 1900 in this *Orbitolina*-bearing layer in the Tesel section allows to date this unit to the late early Aptian (Clavel et al., 2014). The appearance of this echinoid genus seems to be a morphological adaptation to the late early Aptian drowning episode, which postdates the last urgonian deposits all around the Vocontian basin (e.g., Frau et al., 2018a; Pictet, 2016; Pictet et al., 2015, 2019).

According to Heim and Baumberger (1933), the Drusberg Member is very thick in the most south eastern anticlinal where the Frümsner Alp and Alp Wis outcrops are situated, reaching about 50 m and more (Fig. 14B). Following the sections, a green glauconitic limestone and associated phosphatic conglomerate is observed at the base or near the middle of the Drusberg Member (e.g., Heim & Baumberger, 1933), overlaying a well-developed firmground. The collected ammonites date from the late *T. vandenheckii* Zone—*G. sartousiana* Subzone and allow to attribute this glauconitic bed to the Chopf Bed (Fig. 14C; Pictet et al., 2022). Due to their position above the Chopf Bed, the overlying upper Drusberg marlstones correspond to the Lower Hurst Beds of the Alvier region (Briegel, 1972), which we labelled D2 in Pictet et al. (2022). Ammonites from the *G. sartousiana* Subzone date this unit (Pictet et al., 2022) which likely extends upward to the lower *M. sarasini* Zone toward the Rhine valley, where the Schrattenkalk platform unravels in the Drusberg Member. Heim (1905) and Heim and Baumberger (1933) noticed that the Rawil Member is absent in the eastern part of the Alpstein massif but were not able to explain this absence. In our opinion, the absence in the eastern regions can be explained by the later south eastward progradation of the Schrattenkalk platform over deeper environments. The Rawil Member is represented by sedimentary series of marly hemipelagic facies (Upper Hurst Beds; Briegel, 1972), integrated in the Drusberg Member, whereas the Schrattenkalk Formation is represented only by its younger part (unit S3). A half shell of a large *Martelites martelli* Conte, 1989 (Fig. 11C) was collected in 1973 in Brau (Bezau, Austria), 25 km east from the Alpstein massif, which original level of this ammonite is unknown. This latest Barremian ammonite supports a younger age of the upper Drusberg series in the eastern Rhin valley.

The neritic macrofauna collected in unit S3, like in the tilted block of Langtal—Säntis, does not allow differentiation between a late Barremian and an early Aptian age. To resolve this uncertainty, further studies of the ammonite fauna of hemipelagic sedimentary

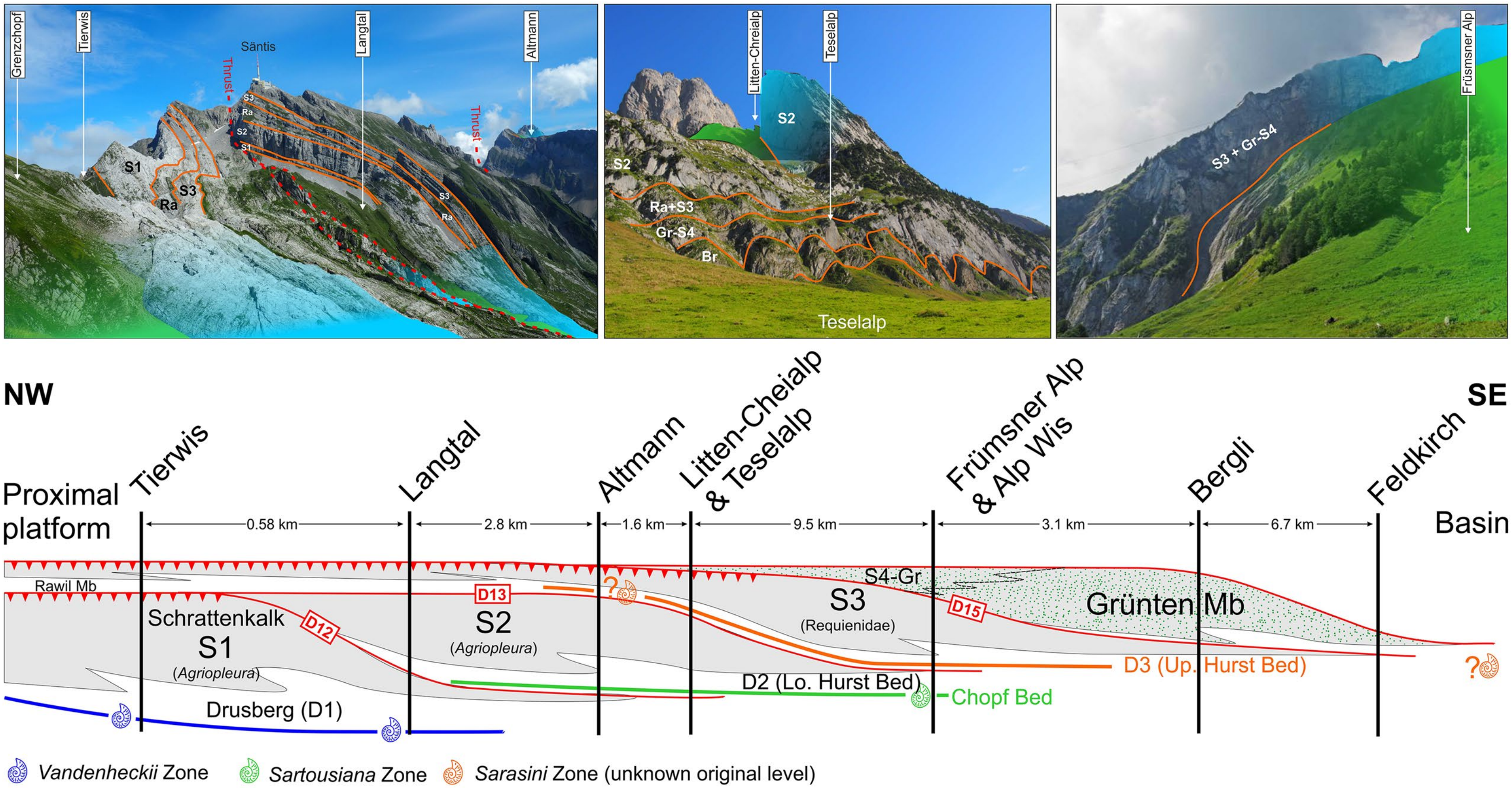

Fig. 15 Not to scale two-dimensional schematic platform-to-basin transect showing the successive platform developments between Tierwis and Feldkirch and interpreted panoramic views supporting this sedimentary model. Ra = Rawil Mb, Gr = Grünten Mb, Br = Brisi Mb, S1 to S3 = Schrattenkalk units, D1 to D3 = Drusberg units. The distances indicated between the sections are actual distances and not palinspastic distances

series equivalent to the Rawil and the "upper" Schrattenkalk members are needed, e.g. in the Werdenberg massif (canton of St.Gallen) and the Brienzergrat (cantons of Berne, Lucerne and Obwalden). In the meantime, a review of the few ammonites collected in the Schrattenklak Formation of central Switzerland is given in chapter 5.3.

5.1.4 Summary of the field observations about the Schrattenkalk Formation in the Alpstein massif

In most proximal platform settings of the Alpstein massif like in Tierwis, the onset of the first carbonate platform progradation phase (forming the unit S1) starts in the late Barremian (*T. vandenheckii* Zone). The second progradation phase (unit S2) is missing there. Instead, the third progradation phase (unit S3) and together with the transgressional Rawil Member are superposed directly on the unit S1, separated by a conspicuous karstic surface and associated shore deposits. In the middle ranges of the Alpstein massif like in the Langtal-Säntis bloc, the three platform progradation phases (units S1, S2, and S3) are superimposed vertically and from northwest to southeast (see Fig. 15), with a very reduced unit S1. Units S2 and S3 are separated by a remarkable brown to grey marlstone-limestone bundle, characteristic for the Rawil Member. In the eastern range like in Litten-Chreialp and Teselalp, the first carbonate platform progradation phase (unit S1) is completely replaced by the distal shelf Drusberg facies and the phosphate and glauconite-bearing Chopf Bed. This Bed itself is overlain by the upper series of the Drusberg Member, corresponding to the Lower Hurst marls of the Alvier region (Briegel, 1972).

A more echinodermic and slightly glauconitic carbonate unit S4-Gr is observed atop the Schrattenkalk succession in the eastern sections. It marks a new progradation phase of the platform, separated from the unit S3 by the intermediary of a firmground surface (D15).

5.2 Lithostratigraphic implications

For more than a century the Schrattenkalk Formation has been thought to be composed of two units, the "Lower" and the "Upper" Schrattenkalk, separated by the more marly Rawil Member. New field observations question this dichotomy. A first bimodal lithostratigraphic cut of the Schrattenkalk Formation was introduced by Kaufmann (1867) following the absence versus the presence of rudist shells (Fig. 2). It was quickly abandoned in favour of the Lower and Upper Schrattenkalk units in the sense of Heim, (1910–1916), separated by the "*Orbitolina* marls". The lithostratigraphic subdivision of the Schrattenkalk Formation was criticised by Bollinger, (1988), at least for the eastern Swiss region. He proposed to abolish the terms "lower" and "upper" and to keep only a Schrattenkalk Member (= Schrattenkalk Formation in the current sense; see also Jost-Stauffer, 1993). Such a dichotomy is also problematic in the most proximal areas where the Rawil Member presents purely carbonated facies (Schenk, 1992), forming in total an enormous uniform rock wall.

More recently, Wissler, (2001) and Wissler et al. (2003) documented the Schrattenkalk Formation within a section along the western flank of the Zuestoll peak, in the Churfirsten, 10 km south of our working area (coord: 2′739′870/1′224′320 to 2′739′950/1′224′770). They identified three sedimentary cycles (P1, P2 and P3) inside the Schrattenkalk Formation that reflect three phases of platform progradation separated by exposure and/or transgressive facies. Such sediments could potentially be interpreted as "*Orbitolina* beds" separating some Schrattenkalk cliff-forming units despite different stratigraphical positions. Following Huck et al., (2013, p. 171: "*Palorbitolina mass occurrences are interpreted as regional expressions of an increasing nutrient influx related to accelerated hydrological cycling, presumably combined with an oscillating sea-level*") orbitolinid beds thus can occur at various stratigraphical levels within the Barremian stage. Wissler et al. (2003) correlated the discontinuity surface observed between their platform progradation cycles P1 and P2 with the glauconitic Chopf Bed and the second transgression phase observed at the base of their cycle P3 with the Rawil Member.

Our biostratigraphic data as well as bedding patterns, facies architecture and bounding surfaces in the Schrattenkalk Formation suggest that the carbonate production mode is a typical ramp-type platform with low-angle oblique clinoforms. Because of the lack of frame-building organisms, the sedimentation is dominated by bioclastic carbonates with stratal patterns like those described from siliciclastic shelves, a common feature of the urgonian platforms (Hunt & Tucker, 1993). The series related to the Schrattenkalk platform sensu stricto were developed in a succession of three carbonate bodies (S1 to S3, Fig. 15). These lenses are arranged following a progradation phase (S1 to S2), followed by an aggradation-progradation phase (S2 to S3). Wissler's studies of the Churfirsten (Wissler, 2001; Wissler et al., 2003) allow us to affirm that the Churfirsten and the Alpstein mountain ranges present the same Schrattenkalk platform succession with three platform progradation phases, each of contemporaneous age.

The question arises if cartographers are able to differentiate between the successive marly bundles intercalated in the Schrattenkalk Formation, although specialised researchers are fighting about their age attribution and

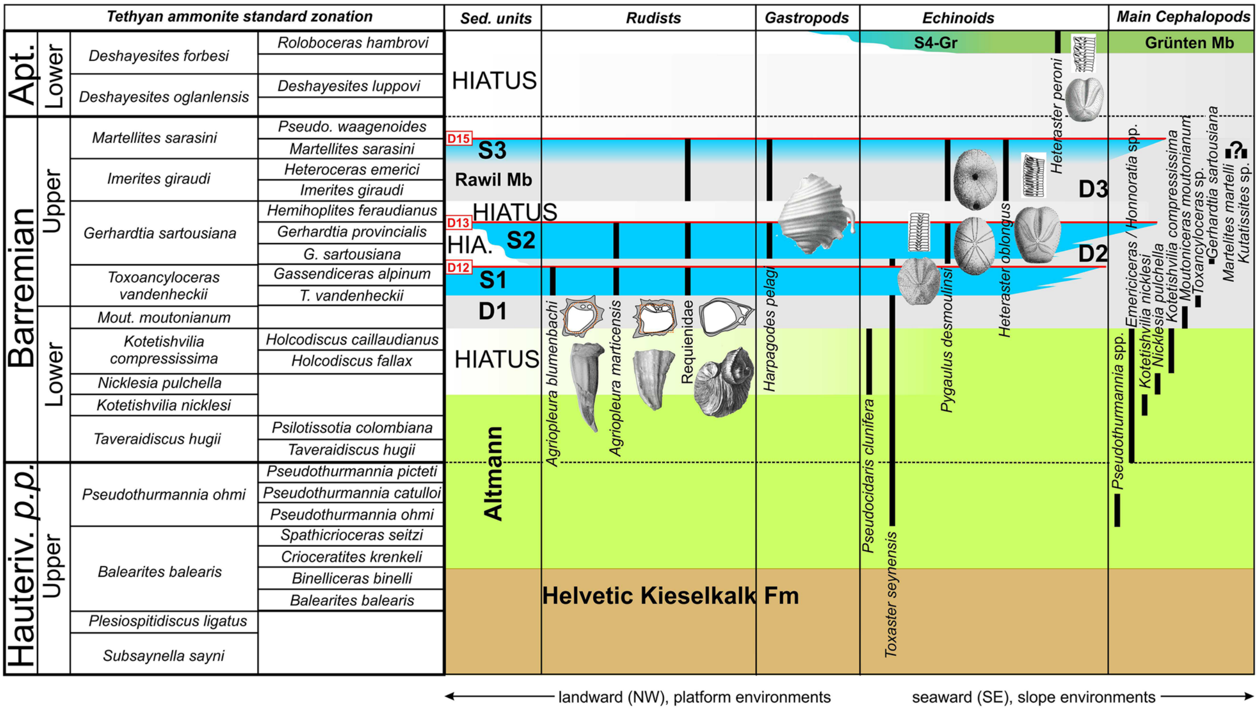

Fig. 16 Time–space diagram of the upper Hauterivian to lower Aptian sedimentary succession in the Alpstein massif. The proximal settings of the Schrattenkalk platform are situated on the left and the slope deposits of the Tierwis Formation are on the right. S1–S3 = units of the Schrattenkalk Formation, D1–D3 = units of the Drusberg Member of the Tierwis Formation Standard Mediterranean ammonite zonation modified after Reboulet et al. (2018). Rudist-shells drawings from Matheron (1842) and from Pictet and Campiche (1868–1871). Rudist-cross sections modified after Masse and Fernerci-Masse (2015). *Harpagodes* drawing from Pictet and Renevier (1854–1858). Echinoids drawings from Pictet and Renevier (1858), de Loriol (1873) and Lambert (1920). Ambulacral pores drawings from Clavel in Charollais et al. (2009) and from Clavel et al. (2014)

stratigraphic position. We suggest to be very careful when attributing a lithostratigraphic rank to the cliff units composing the Schrattenkalk Formation.

The topmost unit S4-Gr rises problems in term of lithostratigraphy. The unit is a light-coloured limestone visually very similar to the Schrattenkalk Formation in the Altmann sections. It is characterised by a more echinodermic and slightly glauconitic limestone. Rudist shells of the genus *Toucasia* Munier-Chalmas, 1873 are even observed in the Tesel section. Because of its lithological similarity with the Schrattenkalk limestone, Heim (1905) named this unit "Schrattenkalk-Echinodermenbreccie". Heim and Baumberger (1933, p. 212) called it "glauconitischer Schrattenkalk (Grüntenschichten)" and noticed that this unit was a possible lateral equivalent of the Grünten Member. In facts, the unit S4-Gr thickens and enriches in orbitolinids towards the Rhein valley and presents no more rudist shells. It becomes mappable south eastward from the Tesel section, from where it becomes clear that this unit is contemporaneous with the Grünten Member of central and western Swiss Alps. For reminder, Linder et al. (2006) excreted the Grünten Member from the Schrattenkalk Formation because of the presence of phosphate-bearing beds. However, up to now, no phosphatic beds were observed in our unit S4-Gr of this region. The Grünten Member is considered as late early Aptian in age by Linder et al. (2006), a dating which is in agreement with the biostratigraphical markers of our unit. Moreover, the unit S4-Gr is attributed to the Grünten Member by Funk et al. (2000). However, in the Alpstein, the unit S4-Gr presents intermediate sedimentological and paleontological characters between the Schrattenkalk Formation ant the Garschella Formation, which makes it difficult to classify in term of lithostratigraphy, at least for its most proximal occurrences.

5.3 Key beds and ammonite bio-events

A succession of marker-surfaces and beds observed within or at the boundaries of the Schrattenkalk Formation is associated or correlated with: (i) positive excursions in oceanic phosphorus burial; (ii) notable carbon isotope fluctuations with negative and following positive excursion; (iii) condensed intervals sometimes combined with important phosphate authigenesis; (iv) ammonite accumulations and bio-events. These surfaces and beds are interpreted as the result of drowning episodes. Our revised calibration substantially modifies the dating of the drowning phases within the upper Barremian Schrattenkalk Formation. Three events of regional significance are recognized.

5.3.1 "Sartousiana" event

The *"Sartousiana*" event was discussed in Pictet et al. (2022) regarding to slope environments. We discuss here how this event affects the neritic platform environments of the Schrattenkalk Formation.

This event is associated to the discontinuity surface D12 (Figs. 9, 10, 14), a remarkable sedimentary event, which constitutes a well-marked time-line crossing in our platform-to-basin transect (Figs. 15, 16). In the distal platform setting, this same discontinuity surface D12 is associated to a glauconite and phosphate-rich conglomerate, the Chopf Bed (Fig. 14C). This bed is situated inside the Drusberg Member and corresponds to the uppermost *T. vandenheckii* Zone and lowermost *G. sartousiana* Zone according to Bodin et al. (2006a). Landwards like in Litten-Chreialp and Altmann sections, the Chopf Bed overlays the clinoform packages of the Schrattenkalk unit S1 (Fig. 10B). In shallower environments represented by the Langtal-Säntis section, the discontinuity D12 overlies a 10 m-thick unit S1, which is incorporated within the base of the Schrattenkalk cliff. The discontinuity surface presents a sharp lithological break associated with a prominent facies change large enough to be observed from afar (Fig. 9D). In the Tierwis-Grauchopf area, representing the most proximal platform setting, the discontinuity D12 is combined with the discontinuity D13 atop the unit S1, which represents the total thickness of the lower cliff. The discontinuity surface is a pronounced karstic surface, developed only along the north-western range (Fig. 4E). The surface records a drop of 2‰ in $\delta^{13}C$ just below it (Fig. 8). This negative isotopic peak must be regarded as the diagenetic imprint of the exposure. It cannot be correlated with any negative excursion in the pelagic record contrary to the interpretation of Stein et al., (2012a, 2012b) and Bonvallet et al. (2019). The macrofauna, present on both sides of the exposure surface, indicates that the entire *G. sartousiana* Zone is missing in this area.

5.3.2 Taxy event

The discontinuity D13 (Figs. 5, 8, 9, 10, 12) corresponds in the Alpstein massif to a regional exposure of the proximal carbonate platform associated with the last occurrence of the rudist genus *Agriopleura*. This pseudotermination of the genus *Agriopleura* was pointed out on the various urgonian carbonate platforms bordering the Vocontian basin and called the "*Agriopleura* event" by Masse and Fenerci-Masse (2013a, b, 2015) and Masse et al. (2020). This event is assigned to the *G. provincialis*–*H. feraudianus* subzonal boundary (Frau et al., 2018a). Orbitolinid foraminifera were also strongly impacted with a drastic diversity decrease (Clavel et al., 2014). Echinoids equally present a turn-over with the replacement of the neritic species *Heteraster couloni* (Agassiz, 1839) by *H. oblongus* (Brongniart, 1821) and the hemipelagic species *Toxaster seynensis* (Lambert, 1920) by *T. colleignoi* (Sismonda, 1843) (see Clavel et al., 2014). Following Masse and Fenerci-Masse (2015) and Masse et al. (2020), this biological crisis of the carbonate platform coincides in time with climatic cooling, increasing sea-water fertility, modifications in deep-sea bottom circulation, platform perturbations including exposure and basin margin instability.

The discontinuity surface D13 indicates a remarkable sedimentary change from coral and rudist-bearing Urgonian-type series to a mixed siliciclastic–carbonate depositional system (Rawil Member = Lower Orbitolina Beds; Marne à *Heteroceras* of Paquier, 1900 *pro parte*; Vire à *Heteroceras* "VH" of Ferry, 2017). This sedimentary change constitutes a well-marked stratigraphical interval visible through our platform-to-basin transect (Figs. 15, 16). The series of the Rawil Member very often present a transgressive system tract composed of several superposed shallowing-upward parasequences showing features of exposure at their top (Bonvallet et al., 2019; Stein et al., 2012a). In the Tierwis-Grauchopf sections, two prominent marly episodes are recorded. The first level situated one metre above the exposure surface (Figs. 5A–C) is here characterized by a mass occurrence of the gastropod *Harpagodes pelagi* (Brongniart, 1821) and by charophytes. The second marly layer at the top of the Rawil Member overlays a strongly bioturbated surface, which is characterized by the mass occurrence of *Palorbitolina lenticularis* (Blumenbach, 1805) in association with the echinoid *Heteraster oblongus* (Brongniart, 1821) (Figs. 5E–F and 6B). Between the two marly layers, typical urgonian series with rich coral carpets and rudist-bearing carbonates are intercalated. Stein et al., (2012a, pp. 955–956) observed these two transgressive episodes on a larger scale across the Helvetic domain, characterised by circalittoral, deeper-water assemblages and the abundance of echinoderms. They interpret the upper marly episode as the maximum flooding surface, which is in accordance with the appearance of a diversified echinoderm fauna in the Tierwis-Grauchopf section. Two successive transgressive parasequences are also recorded in the Jura domain (Pictet, 2021; Pictet et al., 2019). In the latter area, a lower charophytes-bearing marly intercalation contains brackish to freshwater facies and yielded abundant microfossils of latest Barremian age. An upper

Fig. 17 *Martelites* sp., foundation works of the Hotel Metropol at Brunnen in the 60 s, Eidgenössische Technische Hochschule Zürich, cat. no. eth27789, "upper" Schrattenkalk. Umbillical and oblique view of the imprint and cross section (in black) with extrapolated parts in grey colour

marly layer with abundant *Heteraster oblongus* (Brongniart, 1821) represents open-marine facies.

Sedimentary series corresponding to the Rawil Member were originally assigned to the lowermost part of the Aptian stage by Renevier (1877, 1881, 1890) based on the macrofaunal assemblage, an age followed until today. Following Renevier, "*Pterocera*" *pelagi* (Brongniart, 1821), *Heteraster oblongus* (Brongniart, 1821), *Orbitolina lenticularis* (Blumenbach, 1805) and "*Reqienia Lonsdali*" (Sowerby, 1837) are typical species of its Rhodanian stage (Renevier, 1877; i.e., = early Aptian) previously described in the Perte-du-Rhône (Jura mountains, Renevier, 1855). The age of this Jura fauna is revised in Pictet et al., (2016, 2019). The early Aptian age of the Rawil Member was later supported by the cooccurrence of ammonites from the Chartreuse and Vercors massifs (French Subalpine ranges; Arnaud et al., 1998; Gidon, 1952; Moret & Deleau, 1960) referred to *Ancyloceras* gr. *matheronianum* Orbigny, 1842 and *Deshayesites* gr. *weissi* (Neumayr & Uhlig, 1881) but never described and only partially figured. Both specimens are discussed in Frau et al., (2018a, p. 243) and attributed to the latest Barremian. In the Helvetic domain, a few ammonites from the Rawil Member and from the "upper" Schrattenkalk are cited in the literature. Fichter (1934) signalled a very worn fragment in the Rawil Member of the Bauen-Brisi area, which unfortunately is missing in his material and considered as lost or never collected. Lienert (1965, pp. 78 and 128) reports a *Procheloniceras* sp. from the

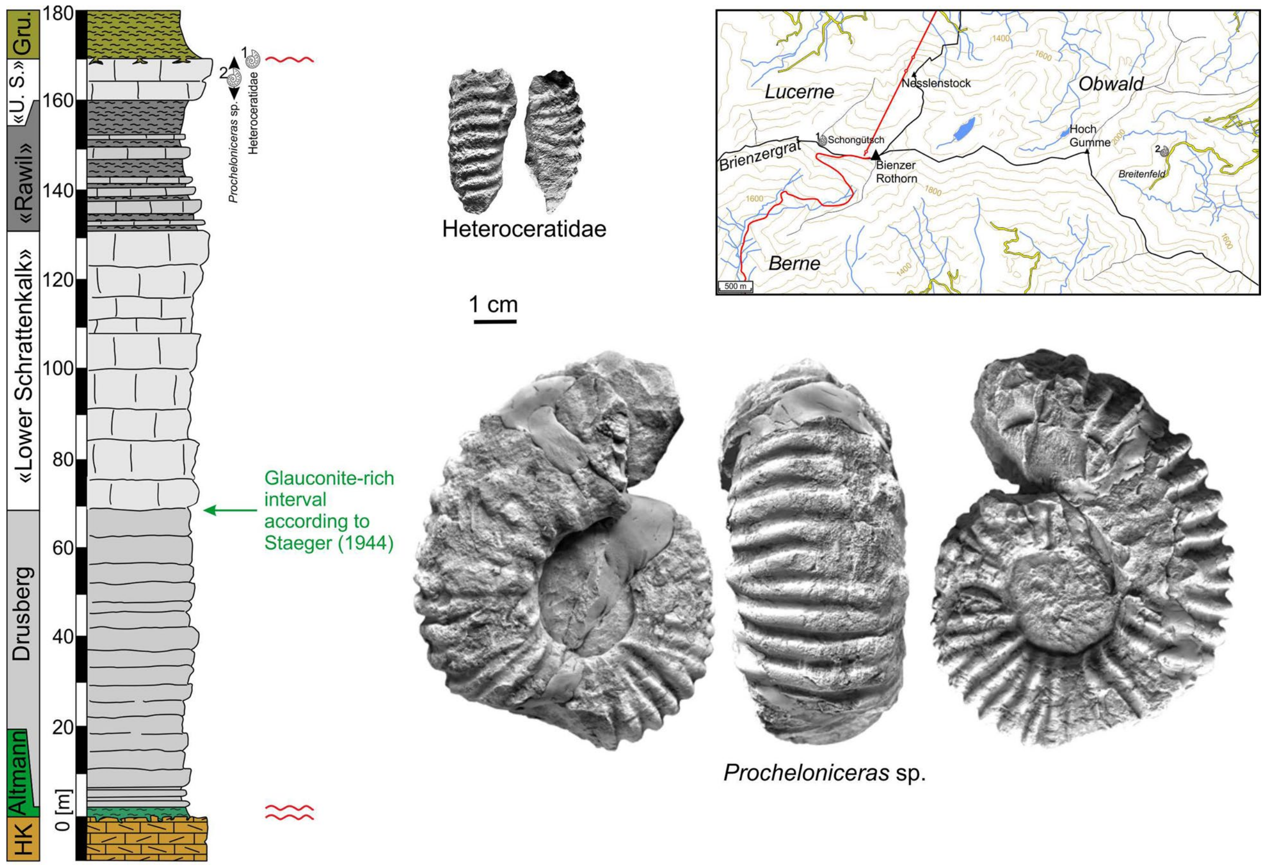

Fig. 18 Stratigraphic log of the Schongütsch section (Brienzergrat, cantons of Lucerne) modified after Jost Stauffer (1993). Heteroceratidae collected by Jost Stauffer (1993) on top of the "Schrattenkalk" Formation, cat. no. 125, Coll. Jost Stauffer, University of Bern. *Procheloniceras* sp. collected by Staeger (1944) in the "upper Schrattenkalk" Formation at Alp Breitenfeld, Coll. Staeger, University of Bern

upper Schrattenkalk of Brunnen, stored in the collections of ETHZ. The genus *Procheloniceras* Spath, 1923 is present as well in the uppermost Barremian than in the lowermost Aptian record. Lienert (1965, p. 22) also mentions large Aptian *Parahoplites* specimens from the upper Schrattenkalk of Brunnen. A corresponding 35 cm large counter print of an ammonite from Brunnen was found in the ETHZ collections (Fig. 17; n coll eth27789). This very evolute to nearly advolute specimen shows backward inclined and straight ribs as well as relatively flattened sides, which are typical for the genus *Martelites* Conte, 1989. This genus characterises the uppermost Barremian *M. sarasini* Subzone, in accordance with the co-occurrence of the genus *Procheloniceras* Spath, 1923. Furthermore, Staeger (1944) collected in the "upper Schrattenkalk" of Alp Breitenfeld, in the Brienzer Rothorn massif, a complete specimen of *Procheloniceras seminodosum* (Sinzow, 1906) (presently assigned as *P.* sp. pending the specimen review; Fig. 18). Finally, Jost-Stauffer (1993) collected, at the top of the "upper Schrattenkalk", a fragment of an ammonite on the Schöngutsch section in the Brienzer Rothorn summit (Fig. 18). This fragment was originally determined by R. Busnardo in 1993 as *Deshayesites* sp. (Jost-Stauffer, 1993, p. 35). This fragment shows a typical rectangular to squared cross-section and ribbing style with oblique orientation on the venter that allows to revise it as a part of an Heteroceratidae indet. All these ammonites' discoveries point to a latest Barremian (*M. sarasini* ammonite Subzone) for the"upper" Schrattenkalk. By the way, a major ammonoid turnover at the base of the *Imerites giraudi* Zone was reported by Vermeulen (2005), characterized by the diversification of Heteroceratidae and a gradual replacement of the Hemihoplitidae and Barremitidae by the diversifying Ancyloceratidae.

Thus, all these paleontological data point to an uppermost Barremian age for the Rawil Member. These observations are in accordance with the worldwide reported occurrence of laminated, organic-rich muds in basinal environments during the latest Barremian. These latest Barremian LOMs were particularly studied in the la

Bédoule section and named as "Taxy Episode" by Föllmi (2012).

5.3.3 Final demise of the Schrattenkalk platform

An important unconformity is located between the Schrattenkalk and the Garschella formations indicating the end of the rudist-bearing shallow-water carbonate platform sedimentation. This unconformity as well as the overlaying sediments show a strong differentiation along the platform-to-basin transect. In distal parts of the platform, like in Schlatt-Mätzenacker and Tesel Alp, the Schrattenkalk Formation ends with a discrete corrugated and bored hardground topped by the lower Aptian Grünten Member or by the unit S4-Gr (Fig. 14F–G). In the Altmann section, the Schrattenkalk Formation is topped by a reduced—unit S4-Gr and/or by a reduced upper Aptian Brisi Member by the intermediary of a shallow to a deep unconformity. In proximal platform parts, like in Langtal and Tierwis, the Schrattenkalk Formation ends with a very irregular and corroded surface, associated to locally brecciated epikarstic cavities, and karstic fissures (Fig. 7A, C). The top of the Schrattenkalk Formation is missing due to extensive and repeated erosion during later successive eustatic cycles. The Schrattenkalk is capped by the middle Albian Sellamatt Beds (Selun Member, Garschella Formation). Thus, the discontinuity surface shows a more and more corroded surface toward the land, passing from a bored hardground to a strongly karstified surface. The surface is covered by younger sediments toward the proximal platform, comprising an increasing time duration of the associated hiatus. This sedimentary story seems to occur throughout the Helvetic domain (Föllmi, 2008).

The onset of the final drowning phase of the Schrattenkalk Formation cannot be dated precisely in the Alpstein massif. However, the distal platform sections like Tesel Alp, where the hiatus has the least duration, indicate that platform drowning occurred before the deposition of the upper lower Aptian unit S4-Gr/Grünten Member. The previously discussed age arguments for the Rawil Member and above Schrattenkalk unit S3, as well as the rare ammonites from central Switzerland, indicate that the Schrattenkalk demise occurred during or just after the *M. sarasini* Zone. We therefore conclude that it occurred somewhere between the latest Barremian *M. sarasini* Zone and the middle early Aptian.

The Urgonian carbonate platform demise is regarded as of global importance by Föllmi (2008). It is recorded all along the peri-Vocontian platforms by a subaerial exposure like on the North Provence platform (Léonide et al., 2012, 2014; Masse & Fenerci-Masse, 2011), the Languedoc platform (Pictet et al., 2015), the Vercors platform (Arnaud-Vanneau et al., 2005; Moss & Tucker, 1996), the Jura platform (Charollais et al., 1994; Pictet et al., 2016, 2019) and the Helvetic platform (Bonvallet et al., 2019; Pictet, 2016). Because its previous dating from the middle early Aptian, the final demise has been believed to be the result of an important phase of paleoenvironmental change related with the early Aptian oceanic anoxic event (OAE 1a: "Selli event"; e.g., Föllmi, 2008; Föllmi & Gainon, 2008; Schlager & Philip, 1990; Wissler et al., 2003). Age control obtained by Föllmi (2008) and Föllmi and Gainon (2008) in the Helvetic domain suggested that the onset of platform demise slightly preceded OAE 1a. This delay was regarded as the expression of a lead-lag effect. Based on cyclostratigraphic calibration of basinal sections, Huck et al. (2011) have established a time gap of about 300 kyr between the Helvetic platform drowning and OAE1a. Thus, these authors suggested that the causal relationship between these two events had to be re-considered. However, the recent revised dating of Urgonian carbonate platforms show that the demise predates the OAE 1a of at least 1 Myr (Frau et al., 2020). Frau et al. (2020) suggested that this large-scale exposure event may have resulted from a relative sea-level fall of high amplitude, resulting from a short-lasted global cooling phase associated with glacio-eustasy.

5.4 Preludes to the OAE1a event

Föllmi (2012) and students considered the Barremian time interval and more particularly the late Barremian-earliest Aptian to have been a period of relative stability in the evolution of the biosphere. These conditions allowed the development of extensive Urgonian platforms on the north-western Tethyan margin, which were particularly favourable during the late Barremian (Bonvallet et al., 2019). Following Bodin et al. (2006b), Godet et al. (2010), Föllmi and Godet (2013) and Bonvallet et al. (2019), a long-term decreasing trend in detrital and phosphorus contents took place during the late Barremian as weathering rates lowered on the adjacent continents and nutrient levels decreased in the surrounding seas, which enabled the late Barremian pulse in the development of the Urgonian shallow-water carbonate platform.

However, the hypothesis that the late Barremian-early Aptian time interval had been a period of relative stability in the evolution of the biosphere is challenged by the revised dating of the peri-Vocontian platforms (e.g., Frau et al., 2018a; Pictet, 2021; Pictet et al., 2019) and by this study. Furthermore, organic rich shales were reported worldwide in the upper Barremian sedimentary series while they are nearly absent in the lowermost Aptian records. A series of black shales were observed in the *T. vandenheckii*, *G. sartousiana* and *I. giraudi-M. sarasini* zones respectively in the Lower Saxony Bassin (Hoffmann

& Mutterlose, 2011; Malkoč & Mutterlose, 2010; Mutterlose & Böckel, 1998; Mutterlose & Bornemann, 2000; Pauly et al., 2013), in the central Tethys (Cecca & Landra, 1994; Frau et al., 2016; Landra et al., 2000; Sprovieri et al., 2006), partially in the Vocontian basin area like in La Bédoule (SE France; Frau et al., 2016; Masse & Fenerci-Masse, 2011; Masse & Machhour, 1998; Stein et al., 2012b) and in southern Spain (Aguado et al., 2014). Further black shales occurrences were also observed in the central and northern Atlantic as observed in DSDP and ODP sites (Stein et al., 1988; Weissert, 1981). Thus, a succession of short and repeated periods of dysaerobic to anaerobic conditions, associated to the deposition of a succession of pelagic organic-rich deposits took place during the late Barremian with particularly enhanced occurrences during the *G. sartousiana* Zone and the *I. giraudi*–*M. sarasini* zones.

It appeared that, in the Alpstein mountains, the Schrattenkalk Formation is interspersed with two sedimentary events associated to higher phosphorus values and to mixed photozoan—heterozoan assemblages, marked by significant quantities of flat orbitolinids and annelids (Bonvallet et al., 2019; Wissler et al., 2003), the "Sartousiana" event and the Taxy event respectively. The "Sartousiana" event is dated to the uppermost *T. vandenheckii* Zone and lowermost *G. sartousiana* Subzone (Pictet et al., 2022). The Taxy event is dated from the *I. giraudi* and lower *M. sarasini* zones (Frau et al., 2016; Masse & Fenerci-Masse, 2011). This dating is in accordance with the few ammonites of latest Barremian age collected in the "upper" Schrattenkalk and distal counterparts. The "Sartousiana" and the Taxy events are interpreted as the result of drowning phases, which both may coincide in time with large scale changes in the ocean-climate system.

In fact, the latest Barremian-early Aptian time interval is globally characterized by large fluctuations in palaeoceanographic, paleoenvironmental, and palaeobiological conditions (Aguado et al., 2014). Increased seafloor spreading and an increased submarine volcanic activity of the Ontong-Java Plateau led to a high sea level and intense volcanic outgassing (e.g., Erba et al., 2015). This contributed to the onset of a widespread greenhouse climate and to a major perturbation in the global carbon cycle (Aguado et al., 2014; Erba, 1994; Föllmi, 2012; Huck et al., 2013; Larson, 1991; Leckie et al., 2002; Mehay et al., 2009; Skelton, 2003; Tejada et al., 2009). These conditions induced high primary productivity, favouring the largely distributed deposition of organic-rich sediments. It culminated in the worldwide early Aptian Selli episode (OAE1a; Coccioni et al., 2003; Erba et al., 2015; Föllmi, 2012) and, together with a dense succession of "mid-Cretaceous" oceanic anoxic events, representing a major phase of paleoenvironmental change (Aguado et al., 2014; Arthur et al., 1990; Erba, 1994; Jenkyns, 1980, 2003, 2010; Larson & Erba, 1999; Leckie et al., 2002).

6 Conclusions

We revised the dating of the Schrattenkalk Formation in the Alpstein massif and analysed bedding patterns, the facies architecture, and bounding surfaces of the formation. Based on these data, we suggest that the carbonate production mode is a typical ramp-type platform with low-angle oblique clinoforms. The stratal patterns are dominated by bioclastic carbonates which deposited in the same way as in siliciclastic shelves, a common feature of the urgonian platforms. In contrast to the actual subdivision of the Schrattenkalk into a lower and an upper part, separated by the Rawil Member, we postulate that the Schrattenkalk series developed in a succession of three carbonate platform progradation phases, each offset being bounded by an exposure surface and subsequent drowning, while in the distal shelf, condensed ammonites-bearing series have been deposited. The drowning episodes could potentially be interpreted as successive *Orbitolina*-rich beds. The development phases of the platform started with a progradation phase (units S1 to S2) followed by an aggradation-progradation phase (units S2 to S3). The onset of the Schrattenkalk carbonate platform is progressive, showing a SE-directed progradation over time. The oldest neritic deposits of our platform-to-basin transect correspond to the *T. vandeheckii* Zone. The younger carbonates are attributed with uncertainties to the *M. sarasini* Subzone. The lower platform interruption is related to the "Sartousiana" event by correlation with the Chopf Bed on the platform slope. The Rawil Member marks the second platform carbonate interruption and is linked to the Taxy event. Ammonites with uncertain stratigraphic position in the Alpstein mountains suggest that the Rawil Member could date to the latest Barremian (*H. feraudianus* to *M. sarasini* subzones). This age attribution is affined by ammonite discoveries from the "upper" Schrattenkalk of central Switzerland. Due to our observations, the commonly used bimodal nomenclature of the Schrattenkalk cliffs should be used with caution.

The overlying unit S4-Gr is morphologically similar to the Schrattenkalk limestone in the Alpstein massif and presents a facies intermediate between the Schrattenkalk Formation and the Grünten Member. The unit S4-Gr locally contains small-sized rudist shells of the genus *Toucasia* Munier-Chlamas, 1873 and differs from the Schrattenkalk Formation by the presence of glauconite grains and a higher echinodermic content. It appears south eastward from the Altmann section. The unit S4-Gr dates from the late early Aptian and thus represents the oldest sedimentary deposits of this stage in the Alpstein massif.

The Barremian time interval and more particularly the late Barremian was considered to have been a period of relative quietness in the evolution of the biosphere, allowing the development of extensive Urgonian platforms. However, organic rich shales were worldwide reported in the upper Barremian series and mostly reported from the *G. sartousiana* and *I. giraudi*-lower *M. sarasini* ammonite-zones. These age intervals are in accordance with a few ammonites of late Barremian age observed in the field or stored in museum collections. The "Sartousiana" and the Taxy events are interpreted as the result of drowning periods which may coincide with large scale changes of the ocean-climate system. The latest Barremian time interval is globally characterized by large fluctuations in palaeoceanographic, paleoenvironmental, and palaeobiological conditions which predated the worldwide and dense succession of oceanic anoxic events of the "mid-Cretaceous" period.

Acknowledgements
The authors warmly thank Dr. Toni Bürgin, Director of the Naturmuseum St.Gallen, for his financial support for the realization of this study. The first author is grateful to the Musée cantonal de géologie of Lausanne for having funded its last fieldtrips and the paleontological plaster copies deposited in the Musée cantonal de geology of Lausanne as well as for funding the publication fees. The authors greatly acknowledge the curators of geoscience collections Dr. Toni Bürgin (Naturmuseum St.Gallen), Dr. J. Georg Friebe (Inatura Museum of Dornbirn), Prof. Dr. Alfons Berger (University of Bern), Dr. Iwan Stössel (Swiss Federal Institute of Technology Zurich) and Dr. Walter Etter (Naturhistorisches Museum Basel) for providing access to the collections or helping us in locating specimens. Dr. Jean-Pierre Masse (Aix-Marseille University) is thanked for his opinion on the rudist shells. The reviewers Serge Ferry and Olivier Kempf are acknowledged for their constructive comments, which have helped to improve this manuscript.

Author contributions
All authors participated to the fieldwork, wrote, proofread, corrected, and approved the entire text. All authors read and approved the final manuscript.

Declarations

Consent for publication
All authors read and approved the final manuscript.

Competing interests
The authors declare that they have no competing interests.

Received: 2 October 2022 Accepted: 27 December 2022
Published online: 24 January 2023

References

Aguado, R., de Gea, G. A., & O'Dogherty, L. (2014). Integrated biostratigraphy (calcareous nannofossils, planktonic foraminifera, and radiolarians) of an uppermost Barremian-lower Aptian pelagic succession in the Subbetic Basin (southern Spain). *Cretaceous Research, 51*, 153–173.

Arnaud, H. (2005). Sequence stratigraphy interpretation. In T. Adatte, A. Arnaud-Vanneau, H. Arnaud, M-C. Blanc-Alétru, S. Bodin, E. Carrio-Schaffauser, K. Föllmi, A. Godet, M. C. Raddadi, J. Vermeulen (Eds.), The Hauterivian lower Aptian sequence stratigraphy from Jura platform to Vocontian basin: A multidisciplinary approach. Field-trip of the 7th International symposium on the Cretaceous (September 1–4, 2005) (Vol. 7, pp. 174–179). *Géologie Alpine, Colloques et excursions*

Arnaud, H., & Arnaud-Vanneau, A. (1991). Les calcaires urgoniens des massifs subalpins septentrionaux et du Jura (France): âge et discussion des données stratigraphiques. *Géologie Alpine, 67*, 63–79.

Arnaud, H., Arnaud-Vanneau, A., Blanc-Alétru, M. C., Adatte, T., Argot, M., Delanoy, G., Thieuloy, J.-P., Vermeulen, J., Virgone, A., Virlouvet, B., & Wermeille, S. (1998). Répartition stratigraphique des orbitolinidés de la plate-forme urgonienne subalpine et jurassienne (SE de la France). *Géologie Alpine, 74*, 3–89.

Arnaud-Vanneau, A. (1980). *Micropaléontologie, paléo-écologie et sédimentologie d'une plate-forme carbonatée de la marge passive de la Téthys: l'Urgonien du Vercors septentrional et de la Chartreuse (Alpes occidentales)*. Ph.D. thesis, (pp. 873) University of Grenoble.

Arnaud-Vanneau, A., Arnaud, H., Carrio-Schaffhauser, E., & Raddadi, M. C. (2005). Urgonian deposits and Barremian-early Aptian sequence stratigraphy in the Vercors massif. In T. Adatte, A. Arnaud-Vanneau, H. Arnaud, M-C. Blanc-Alétru, S. Bodin, E. Carrio-Schaffauser, K. Föllmi, A. Godet, M. C. Raddadi, J. Vermeulen (Eds.), The Hauterivian lower Aptian sequence stratigraphy from Jura platform to Vocontian basin: A multidisciplinary approach. Field-trip of the 7th International symposium on the Cretaceous (September 1–4, 2005) (Vol. 7, pp. 97–126). *Géologie Alpine, Colloques et excursions*

Arthur, M.A., Jenkyns, H.C., Brumsack, H.J., & Schlanger, S.O. (1990). Stratigraphy, geochemistry, and paleoceanography of organic carbonerich Cretaceous sequences. In Ginsburg, R.N., & Beaudoin, B. (Eds.), *Cretaceous resources, events and rhythms: background and plans for research,* (vol., 304, pp. 75–119). *NATO ASI Series C*

Baron-Szabo, R. S. (2021). Upper Barremian–lower Aptian scleractinian corals of central Europe (Schrattenkalk Fm., Helvetic Zone, Austria, Germany, Switzerland). *Zootaxa, 4960*(1), 199.

Bersezio, R., Erba, E., Gorza, M., & Riva, A. (2002). Berriasian-Aptian black shales of the Maiolica formation (Lombardian Basin, Southern Alps, Northern Italy): Local to global events. *Palaeogeography, Palaeoclimatology, Palaeoecology, 180*, 253–275.

Bodin, S., Godet, A., Vermeulen, J., Linder, P., & Föllmi, K. B. (2006b). Biostratigraphy, sedimentology and sequence stratigraphy of the latest Hauterivian–early Barremian drowning episode of the Northern Tethyan margin (Altmann Member, Helvetic Nappes, Switzerland). *Eclogae Geologicae Helvetiae, 99*, 157–174.

Bodin, S., Vermeulen, J., Godet, A., & Föllmi, K. B. (2006a). New data on the age of the installation of Urgonian-type carbonates along the northern Tethyan margin: Biostratigraphy of the Chopf Member (Helvetic Alps, eastern Switzerland). *Comptes Rendus Geoscience, 338*, 727–733.

Bollinger, D. (1988). *Die Entwicklung des distalen osthelvetischen Schelfs im Barremian und Früh-Aptian*. Unpublished PhD thesis, (pp. 136) ETH Zürich, Zürich, Switzerland

Bonvallet, L. (2015). *Evolution of the Helvetic Shelf (Switzerland) during the Barremian-Early Aptian: paleoenvironmental, paleogeographic and paleoocianographic controlling factors*. Ph.D. thesis, (pp. 354) University of Lausanne

Bonvallet, L., Arnaud-Vanneau, A., Arnaud, H., Adatte, A., Spangenberg, J. E., Stein, M., Godet, A., & Föllmi, K. B. (2019). Evolution of the Urgonian shallow-water carbonate platform on the Helvetic shelf during the late Early Cretaceous. *Sedimentary Geology, 387*, 18–56.

Briegel, U. (1972). Geologie der östlichen Alviergruppe unter besonderer Berücksichtigung der Drusberg- und Schrattenkalkformation. *Eclogae Geologicae Helvetiae, 65*, 425–483.

Burckhart, C. (1896). Monographie der Kreideketten zwischen Klönthal, Sihl und Linth. *Beiträge Zur Geologischen Karte Der Schweiz, NF, 5*, 205.

Cecca, F., & Landra, G. (1994). Late Barremian-early Aptian ammonites from the Maiolica Formation near Cesana Brianza (Lombardy basin, northern Italy). *Rivista Italiana Di Paleontologia e Stratigrafia, 100*(3), 395–422.

Cecca, F., Marini, A., Pallini, G., Baudin, F., & Begouen, V. (1994). A guide-level of the uppermost Hauterivian (Lower Cretaceous) in the pelagic succession of Umbria-Marche Apennines (central Italy): The Faraoni level. *Rivista Italiana Di Paleontologia e Stratigrafia, 99*, 551–568.

Charollais, J., Clavel, B., Busnardo, R., Conrad, M., Müller, A., & Decrouez, D. (2009). Olistolithes et coulées bioclastiques: Prémices de l'installation de la plate-forme urgonienne aux confins des Bornes et des Aravis (Haute-Savoie, France). *Archives Des Sciences, 62*, 35–70.
Charollais, J., Clavel, B., Schroeder, R., Busnardo, R., & Horisberger, P. (1994). Mise en évidence de l'émersion post-urgonienne et de la lacune du Barrémien-Bédoulien inférieur/moyen dans le Jura neuchâtelois. *Publications Du Département De Géologie Et De Paléontologie De L'université Genève, 14*, 57–80.
Clavel, B., Busnardo, R., & Charollais, J. (1986). Chronologie de la mise en place de la plate-forme urgonienne du Jura au Vercors (France). *Comptes Rendus De L'académie Des Sciences, Série II, 302*(8), 583–586.
Clavel, B., Charollais, J., Busnardo, R., Granier, B., Conrad, M., Desjaques, P., & Metzger, J. (2014). La plate-forme carbonatée urgonienne (Hauterivien supérieure-Aptien inférieur) dans le Sud-Est de la France et en Suisse : Synthèse. *Archives Des Sciences, 67*, 1–97.
Clavel, B., Charollais, J., Conrad, M., Jan du Chêne, R., Busnardo, R., Gardin, S., Erba, E., Schroeder, R., Cherchi, A., Decrouez, D., Granier, B., Sauvagnat, J., & Weidmann, M. (2007). Dating and progradation of the Urgonian limestone from the Swiss Jura to South-East France. *Zeitschrift Der Deutschen Gesellschaft Für Geowissenschaften, 158*(4), 1025–1062.
Coccioni, R., Galeotti, S., & Sprovieri, M. (2003). The Mid-Barremian Event (MBE): the prelude to the OAE1a. *American Geophysical Union Fall Meeting*, abstract #PP41B-0835.
Coccioni, R., Baudin, F., Cecca, F., Chiari, M., Galeotti, S., Gardin, S., & Salvini, G. (1998). Integrated stratigraphic, palaeontological, and geochemical analysis of the uppermost Hauterivian Faraoni Level in the Fiume Bosso section, Umbria-Marche Apennines, Italy. *Cretaceous Research, 19*, 1–23.
Coccioni, R., Luciani, V., & Marsili, A. (2006). Cretaceous oceanic anoxic events and radially elongated chambered planktonic foraminifera: Paleoecological and paleoceanographic implications. *Palaeogeography, Palaeoclimatology, Palaeoecology, 235*, 66–92.
de Loriol, P. (1873). Echinologie helvétique. Description des echinides des terrains crétacés de la Suisse. *Matériaux Pour La Paléontologie Suisse, 6*, 144.
Erba, E. (1994). Nannofossils and superplumes: The early Aptian "nannoconid crisis." *Paleoceanography, 9*, 483–501.
Erba, E., Duncan, R. A., Bottini, C., Tiraboschi, D., Weissert, H., Jenkyns, H. C., & Malinverno, A. (2015). Environmental consequences of Ontong Java Plateau and Kerguelen Plateau volcanism. In C. R. Neal, W. W. Sager, T. Sano, & E. Erba (Eds.), *The origin, evolution, and environmental impact of oceanic large igneous provinces, special paper 511* (pp. 271–303). Geological Society of America.
Eugster, H., Forrer, M., Frohlicher, H., Kempf, T., Schlatter, L., Blaser, R., Funk, H., Langenegger, H., Spoerri, M., & Habicht, K. (1982). Säntis (map sheet 1115), *Geological Atlas of Switzerland 1:25.000*, N. 78. Federal Office of Topography (Swisstopo).
Ferry, S. (2017). Summary on Mesozoic carbonate deposits of the Vocontian Trough (Subalpine Chains, SE France). *Carnets de Géologie-Book 2017/01 (CG2017_BOOK_01)*
Ficheur, E. (1900). Le Crétacé inférieur dans le Massif des Matmatas (Alger). *Bulletin De La Société Géologique De France, 3*(28), 559–596.
Fichter, H. J. (1934). Geologie der Bauen-Brisen-Kette am Vierwaldstättersee und die zyklische Gliederung der Kreide und des Malm der helvetischen Decken. *Beiträge Zur Geologischen Karte Der Schweiz, NF, 69*, 129.
Föllmi, K. B. (2008). A synchronous, middle Early Aptian age for the demise of the Helvetic Urgonian platform related to the unfolding oceanic anoxic event 1a ("Selli event") Comment on the article «Sur la présence de grands foraminifères d'âge aptien supérieur dans l'Urgonien de la Nappe du Wildhorn (Suisse centrale). Note préliminaire» by R. Schroeder, K. Schenk, A. Cherchi & B. Schwizer, Revue de Paléobiologie, 2007, 665–669. *Revue de Paléobiologie,* 27(2), 461–468
Föllmi, K. B. (2012). Early Cretaceous life, climate and anoxia. *Cretaceous Research, 35*, 230–257.
Föllmi, K. B., Bodin, S., Godet, A., Linder, P., & van de Schootbrugge, B. (2007). Unlocking paleo-environmental interaction from Early Cretaceous shelf sediments in the Helvetic Alps: Stratigraphy is the key! *Swiss Journal of Geosciences, 100*, 349–369.
Föllmi, K. B., & Gainon, F. (2008). Demise of the Tethysian Urgonian carbonate platform and subsequent transition towards pelagic conditions: The sedimentary record of the Col de la Plaine Morte aera, central Switzerland. *Sedimentary Geology, 205*, 142–159.
Föllmi, K. B., & Godet, A. (2013). Palaeoceanography of Lower Cretaceous Alpine platform carbonates. *Sedimentology, 60*, 131–151.
Föllmi, K. B., Godet, A., Bodin, S., & Linder, P. (2006). Interactions between environmental change and shallow-water carbonate build-up along the northern Tethyan margin and their impact on the early Cretaceous carbon-isotope record. *Paleoceanography, 21*, 16.
Föllmi, K. B., & Ouwehand, P. J. (1987). Garschella-Formation und Götzis-Schichten (Aptian-Coniacian): Neue stratigraphische Daten aus dem Helvetikum der Ostschweiz und des Vorarlbergs. *Eclogae Geologicae Helvetiae, 80*, 141–191.
Frau, C., Delanoy, G., Masse, J.-P., Lanteaume, C., & Tendil, A. J. B. (2016). New Heteroceratidae (Ammonoidea) from the late Barremian deepening succession of Marseille (Bouches-du-Rhône, France). *Acta Geologica Polonica, 66*(2), 205–225.
Frau, C., Masse, J.-P., Fenerci-Masse, M., Tendil, A.J.-B., Pictet, A., & Lanteaume, C. (2018a). Is Strontium-isotope stratigraphy a reliable tool for dating shallow-marine platform carbonates at the Barremian-Aptian transition? Review of western Tethyan case studies. *Carnets De Géologie, 18*(5), 139–154.
Frau, C., Tendil, A.J.-B., Lanteaume, C., Masse, J.-P., Pictet, A., Bulot, L. G., Luber, T., Refern, J., Borgomano, J., Léonide, P., Fournier, F., & Massonnat, G. (2018b). Late Barremian–early Aptian ammonite bio-events from the Urgonian-type series of Provence, southeast France: Regional stratigraphic correlations and implications for the peri-Vocontian carbonate platforms. *Cretaceous Research, 90*, 222–253.
Frau, C., Tendil, A.J.-B., Pohl, A., & Lanteaume, C. (2020). Revising the timing and causes of the Urgonian rudistid-platform demise in the Mediterranean Tethys. *Global and Planetary Change, 187*, 103124.
Funk, H., Habischt, K. J., Hankte, R., & Pfiffner, A. O. (2000). Säntis (map sheet 1115), *Geological Atlas of Switzerland 1:25.000, N. 78*. Federal Office of Topography (Swisstopo)
Funk, H., & Briegel, U. (1979). The Urgonian facies of the Helvetic nappes in eastern Switzerland. *Géobios, Mémoire Spécial, 3*, 159–168.
Funk, H., Föllmi, K. B., & Mohr, H. (1993). Evolution of the Tithonian-Aptian Carbonate Platform Along the Northern Tethyan Margin, Eastern Helvetic Alps. In T. Simo, R. W. Scott, & J. P. Masse (Eds.), *Cretaceous carbonate platforms* (Vol. 56, pp. 387–407). American Association of Petroleum Geologists.
Gidon, P. (1952). Une ammonite de l'Urgonien en Grande-Chartreuse. *Comptes Rendus Sommaires De La Société Géologique De France, 11*, 237–238.
Godet, A., Föllmi, K. B., Bodin, S., de Kaenel, E., Matera, V., & Adatte, T. (2010). Stratigraphic, sedimentological and palaeoenvironmental constraints on the rise of the Urgonian platform in the western Swiss Jura. *Sedimentology, 57*, 1088–1125.
Godet, A., Föllmi, K. B., Spangenberg, J. E., Bodin, S., Vermeulen, J., Adatte, T., Bonvallet, L., & Arnaud, H. (2013). Deciphering the message of Early Cretaceous drowning surfaces from the Helvetic Alps: What can be learnt from platform to basin correlations? *Sedimentology, 60*, 152–173.
Heim, A. (1910–1916). Monographie der Churfirsten-Mattstock-Gruppe. *Beiträge zur geologischen Karte der Schweiz*, NF 20/1–3, 573.
Heim, A. (1905). Das Säntisgebirge. *Beiträge Zur Geologischen Karte Der Schweiz, NF, 16*(1), 654.
Heim, A., & Baumberger, E. (1933). Jura und Unterkreide in den helvetischen Alpen beiderseits des Rheines (Vorarlberg und Ostschweiz). *Denkschriften Der Schweizerischen Naturforschenden Gesellschaft, 68*, 155–220.
Hoffman, R., & Mutterlose, J. (2011). Stratigraphie und Cephalopodenfauna des Unter-Apt von Alstätte (NRW). *Geologie Und Paläontologie in Westfalen, 80*, 43–59.
Huck, A., Heimhofer, U., Immenhauser, A., & Weissert, H. (2013). Carbon-isotope stratigraphy of Early Cretaceous (Urgonian) shoal-water deposits: Diachronous changes in carbonate-platform production in the north-western Tethys. *Sedimentary Geology, 290*, 157–174.
Huck, S., & Heimhofer, U. (2015). Improving shallow-water carbonate chemostratigraphy by means of rudist bivalve sclerochemistry. *Geochemistry, Geophysics, Geosystems, 16*, 18.

Huck, S., Heimhofer, U., Rameil, N., Bodin, S., & Immenhauser, A. (2011). Strontium and carbon-isotope chronostratigraphy of Barremian-Aptian shoal-water carbonates: Northern Tethyan platform drowning predates OAE 1a. *Earth and Planetary Science Letters, 304*(3–4), 547–558.
Hunt, D., & Tucker, M. E. (1993). Sequence stratigraphy of carbonate shelves with an example from the mid-Cretaceous (Urgonian) of southeast France. *Special Publications of the International Association of Sedimentologists, 18*, 307–341.
Jenkyns, H. C. (1980). Cretaceous anoxic events: From continents to oceans. *Journal of the Geological Society, London, 137*, 171–188.
Jenkyns, H. C. (2003). Evidence for rapid climate change in the Mesozoic-Palaeogene greenhouse world. *Philosophical Transactions of the Royal Society of London, 361*, 1885–1916.
Jenkyns, H. C. (2010). Geochemistry of oceanic anoxic events. *Geochemistry, Geophysics, Geosystems, 11*(3), 1–30.
Jost-Stauffer. M. (1993). Geologische Untersuchungen im Helvetikum des östlichen Brienzergrates (Kreide der Wildhorn-Drusberg-Decke). Diploma thesis, (pp. 136) University of Bern
Kaufmann, F. J. (1867). Geologische Beschreibung des Pilatus. *Beiträge Zur Geologischen Karte Der Schweiz, 5*, 168.
Kempf, T. (1966). Geologie des westlichen Säntisgebirges. *Beiträge Zur Geologischen Karte Der Schweiz, NF, 128*, 81.
Lambert, J. (1920). Note sur quelques échinides du Crétacé inférieur de la Provence. *Notes Provençales Du Dr Adrien Guébhard, 11*, 1–22.
Landra, G., Cecca, F., & Vesicek, Z. (2000). Early Aptian ammonites from the top of the Maiolica and the anoxic "Selli level" (Lombardy, Southern Alps). *Bollottino Della Società Paleontologica Italiana, 39*(1), 29–45.
Larson, R. L. (1991). Latest pulse of earth: Evidence for a mid-Cretaceous superplume. *Geology, 19*, 547–550.
Larson, R. L., & Erba, E. (1999). Onset of the mid-Cretaceous greenhouse in the Barremian-Aptian: Igneous events and the biological, sedimentary, and geochemical responses. *Paleoceanography, 14*, 663–678.
Leckie, R. M., Bralower, T. J., & Cashman, R. (2002). Oceanic anoxic events and plankton evolution: biotic response to tectonic forcing during the mid-Cretaceous. *Paleoceanography, 17*, 13-1–13-29.
Léonide, P., Doublet, S., Masse, J-P., & Borgomano, J. (2008). Modélisation géologique et pétrophysique des réservoirs et des unités d'écoulement dans les carbonates de la plate-forme du Crétacé inférieur (Barrémien-Aptien) de Provence - Stratigraphie et sédimentologie des carbonates d'âge Barrémien - Aptien inférieur de la région des Monts de Vaucluse. *Unpublished report of the Laboratoire de Géologie des Systèmes et des Réservoir Carbonatés*. (197 + 40 pp.) Université de Provence.
Léonide, P., Borgomano, J., Masse, J.-P., & Doublet, S. (2012). Relation between stratigraphic architecture and multi-scale heterogeneities in carbonate platforms: The Barremian-lower Aptian of the Monts de Vaucluse, SE France. *Sedimentary Geology, 265*, 87–109.
Léonide, P., Fournier, F., Reijmer, J. G., Vonhof, H., Borgomano, J., Dijk, J., Rosenthal, M., van Goethem, M., Cochard, J., & Meulenaars, K. (2014). Diagenetic patterns and pore space distribution along a platform to outer-shelf transect (Urgonian limestone, Barremian-Aptian, SE France). *Sedimentary Geology, 306*, 1–23.
Lienert, O. (1965). *Stratigraphie der Drusbergschichten und des Schrattenkalkes im Säntisgebirge unter besonderer Berücksichtigung der Orbitoliniden*. Ph.D. thesis, (pp. 141) ETH Zürich
Linder, P., Gigandet, J., Hüsser, J. L., Gainon, F., & Föllmi, K. B. (2006). The early Aptian Grünten Member: Description of a new lithostratigraphic unit of the Helvetic Garschella Formation. *Eclogae Geologicae Helvetiae, 99*, 327–341.
Mahanipour, A., & Eftekhari, M. (2017). The first record of the mid-Barremian Oceanic Anoxic Event in the Zagros Basin: evidence from calcareous nannofossils. *Journal of Nannoplankton Research, 37*, 106.
Malkoč, M., & Mutterlose, J. (2010). The early Barremian warm pulse and the late Barremian cooling: A high-resolution geochemical record of the boreal realm. *Palaios, 25*, 14–23.
Masse, J-P. (1976). *Les Calcaires urgoniens de Provence. Valanginien-Aptien inférieur – Stratigraphie – Paléontologie – Les paléoenvironnements et leur évolution*. Ph.D. thesis. (pp. 255). University of Aix-Marseille II
Masse, J.-P., & Fenerci-Masse, M. (2013b). *Orgon et la région orientale des Alpilles. Itinéraires, sites et paysages géologiques*. Editions de l'Office de Tourisme d'Orgon, 122
Masse, J.-P. (1995). Lower Cretaceous rudist biostratigraphy of southern France—A reference for Mesogean correlations. *Revista Mexicana De Ciencias Geológicas, 12*(2), 236–256.
Masse, J.-P., & Fenerci-Masse, M. (2008). Time contrasting palaeobiogeographies among Hauterivian-Lower Aptian rudist bivalves from the Mediterranean Tethys, their climatic control and palaeoecological implications. *Palaeogeography, Palaeoclimatology, Palaeoecology, 269*, 54–65.
Masse, J.-P., & Fenerci-Masse, M. (2011). Drowning discontinuities and stratigraphic correlations in platform carbonates. The late Barremian-Early Aptian record of South-East France. *Cretaceous Research, 32*, 659–684.
Masse, J.-P., & Fenerci-Masse, M. (2013a). Bioevents and palaeoenvironmental changes in carbonate platforms. The record of Barremian "Urgonian" limestones of SE France. *Palaeogeography, Palaeoclimatology, Palaeoecology, 386*, 637–651.
Masse, J.-P., & Fenerci-Masse, M. (2015). Evolution of the rudist bivalve Agriopleura Kühn (Radiolitidae, Hippuritida) from the mediterranean region. *Palaeontology, 58*(1), 71–100.
Masse, J.-P., & Fenerci-Masse, M. (2017). Taxonomy and stratigraphy of late Barremian-Albian species of Horiopleura Douvillé (Hippuritida, Polyconitidae) of the Mediterranean and southwestern Asian regions. *Cretaceous Research, 76*, 53–80.
Masse, J.-P., & Fenerci-Masse, M. (2018). Taxonomy and stratigraphy of Early Cretaceous species of Debrunia Masse and Fenerci-Masse (Hippuritida, Monopleuridae) of the Mediterranean region. *Cretaceous Research, 84*, 32–61.
Masse, J.-P., Frau, C., Tendil, A.J.-B., & Fenerci-Masse, M. (2020). Evidence for three successive upper Barremian–lower Aptian rudist faunas in the Urgonian-type deposits of southeastern France and their stratigraphic value. *Cretaceous Research, 115*, 15.
Masse, J.-P., & Humbert, S. (1976). Les échinidés du Crétacé inférieur provençal. *Biostratigraphie Et Paléoécologie. Géologie Méditerranéenne, 3*(1), 45–55.
Masse, J.-P., & Machhour, L. (1998). La matière organique dans la série du stratotype historique de l'Aptien inférieur de Cassis-La Bédoule (SE France). In M. Moullade, G. Tronchetti, & J.-P. Masse (Eds.), *Le stratotype historique de l'Aptien inférieur (Bédoulien) dans la région de Cassis-La Bédoule (S.E. France)* (Vol. 25, pp. 55–62). Géologie Méditerranéenne.
Matheron, P. (1842). Catalogue méthodique et descriptif des corps organisés fossiles du département des Bouches-du-Rhône et lieux circonvoisins. *Extrait Du Répertoire Des Travaux De La Société Statistique De Marseille, 6*, 102–129.
Méhay, S., Keller, C. E., Bernasconi, S. M., Weissert, H., Erba, E., Bottini, C., & Hochuli, P. A. (2009). A volcanic CO2 pulse triggered the Cretaceous oceanic anoxiv event 1a and a biocalcification crisis. *Geology, 37*, 819–822.
Moret, L., & Deleau, P. (1960). Notes de paléontologie savoisienne: Découverte d'ammonites dans le Berrias et l'urgonien des environs d'Annecy (Haute-Savoie). *Travaux Du Laboratoire De Géologie De Grenoble, 36*, 43–44.
Moss, S. J., & Tucker, M. E. (1996). Dolomitization associated with transgressive surfaces—a mid-Cretaceous example. *Sedimentary Geology, 107*, 11–20.
Mutterlose, J., & Böckel, B. (1998). The Barremian-Aptian boundary interval in NW Germany: A review. *Cretaceous Research, 19*, 539–568.
Mutterlose, J., & Bornemann, A. (2000). Distribution and facies patterns of Lower Cretaceous sediments in northern Germany: A review. *Cretaceous Research, 21*, 733–759.
Mutterlose, J., Brumsack, H., Flögel, S., Hay, W., Klein, C., Langrock, U., Lipinski, M., Ricken, W., Söding, E., Stein, R., & Swientek, O. (2003). The Greenland-Norwegian seaway: a key area for understanding late Jurassic to early Cretaceous paleoenvironments. *Paleoceanography, 18*(1), 1010.
Mutterlose, J., Malkoc, M., Schouten, S., Sinninghe Damsté, J. S., & Forster, A. (2010). TEX_{86} and stable $\delta^{18}O$ paleothermometry of early Cretaceous sediments: Implications for belemnite ecology and paleotemperature proxy application. *Earth and Planetary Science Letters, 298*, 286–298.
Mutterlose, J., Pauly, S., & Steuber, T. (2009). Temperature controlled deposition of early Cretaceous (Barremian-early Aptian) black shales in an epicontinental sea. *Palaeogeography, Palaeoclimatology, Palaeoecology, 273*, 330–345.
Oberholzer, J. (1933). Geologie der Glarneralpen. *Beiträge Zur Geologischen Karte Der Schweiz, NF, 28*, 626.

Orbigny (d'), A. (1847–1849). *Paléontologie française. Terrain crétacés IV*. Masson ed. Paris

Orbigny (d'), A. (1853–1855). *Paléontologie française. Terrain crétacés VI*. Echinides irréguliers, 597

Paquier, V. (1900). Recherches géologiques dans le Diois et les Baronnies orientales. *Travaux Du Laboratoire De Géologie De La Faculté Des Sciences De L'université De Grenoble, 5*, 149–556.

Pauly, S., Mutterlose, J., & Wray, D. S. (2013). Palaeoceanography of lower Cretaceous (Barremian–Lower Aptian) black shales from northwest Germany evidenced by calcareous nannofossils and geochemistry. *Cretaceous Research, 42*, 28–43.

Pfiffner, O. A. (1981). Fold-and-thrust tectonics in the Helvetic Nappes (E Switzerland). In K. R. McClay, & N. J. Price (Eds), Thrust and nappe tectonics. *Geological Society, London, Special Publications*, (vol., 9, pp. 319–327). Oxford: Blackwell Scientific Publications.

Pictet, F.J., & Renevier, E. (1854–1858). Description des fossiles du terrain aptien de la Perte-du-Rhône et des environs de Sainte-Croix. *Matériaux pour la Paléontologie suisse, 1*, 184

Pictet, F-J., & Campiche, G. 1858–1871. Description des fossiles du terrain crétacé des environs de Sainte-Croix. *Matériaux pour la Paléontologie suisse*. vol. I Stratigraphie, Céphalopodes (1858–1860, p. 380); vol. II Gastropodes (1861–1864, p. 752); vol. III–IV Pélécypodes (1864–1867, p. 643); vol. IV Pélécypodes (1868–1871, p. 352)

Pictet, A. (2016). *The evolution and demise of aptian carbonate platforms along the northwestern Tethyan Margin (SE France to SW Germany), and their relationship with palaeoclimatic and palaeoceanographic changes*. Ph.D. thesis. (pp. 740). University of Lausanne

Pictet, A. (2021). New insights on the Early Cretaceous (Hauterivian-Barremian) Urgonian lithostratigraphic units in the Jura Mountains (France and Switzerland): The Gorges de l'Orbe and the Rocher des Hirondelles formations. *Swiss Journal of Geosciences, 114*(18), 47.

Pictet, A., Delamette, M., & Matrion, B. (2016). The Perte-du-Rhône Formation, a new Cretaceous (Aptian-Cenomanian) lithostratigraphic unit in the Jura mountains (France and Switzerland). *Swiss Journal of Geosciences, 109*, 221–240.

Pictet, A., Delanoy, G., Adatte, T., Spangenberg, J. E., Baudouin, C., Boselli, P., Boselli, M., Kindler, P., & Föllmi, K. B. (2015). Three successive phases of platform demise during the early Aptian and their association with the oceanic anoxic Selli episode (Ardèche, France). *Palaeogeography. Palaeoclimatology. Palaeoecology, 418*, 101–125.

Pictet, A., Kürsteiner, P., Tschanz, K., & Tajika, A. (2022). Record of a dense succession of drowning events in the Alpstein mountains, north-eastern Switzerland: Part I—the Lower Cretaceous Tierwis Formation (latest Hauterivian to latest Barremian). *Swiss Journal of Geosciences, 115*(21), 31.

Pictet, A., Mojon, P.-O., Matrion, B., Adatte, T., Spangenberg, J. E., & Föllmi, K. B. (2019). Record of latest Barremian-Cenomanian environmental change in tectonically controlled depressions from the Jura-Burgundy threshold (Jura Mountains, eastern France and western Switzerland). *Palaeogeography, Palaeoclimatology, Palaeoecology, 514*, 627–654.

Rat, P. (1965). Rapport sur les faciès Urgoniens. *Mémoires Du Bureau De Recherches Géologiques Et Minières, 34*, 157–159.

Reboulet, S., Szives, O., Aguirre-Urreta, B., Barragán, R., Company, M., Frau, C., Kakabadze, M. V., Klein, J., Moreno-Bedmar, J. A., Lukeneder, A., Pictet, A., Ploch, I., Raisossadat, S. N., Vašíček, Z., Baraboshkin, E. J., & Mitta, V. V. (2018). Report on the 6th International Meeting of the IUGS Lower Cretaceous Ammonite Working Group, the Kilian Group (Vienna, Austria, 20th August 2017). *Cretaceous Research, 91*, 100–110.

Renevier, E. (1890). Monographie des Hautes-Alpes vaudoises. *Matériaux pour la carte géologique de la Suisse, 16*, 562.

Renevier, E. (1855). Mémoire géologique sur la Perte du Rhône. *Nouveaux Mémoires De La Société Helvétique Des Sciences Naturelles, 14*, 1–71.

Renevier, E. (1877). Notice sur ma carte géologique de la partie sud des Alpes vaudoises et régions limitrophes. *Archives Des Sciences Physiques Et Naturelles, 2*(59), 45.

Renevier, E. (1881). Sur la composition de l'étage urgonien. *Bulletin De La Société Géologique De France, 3*(9), 618–619.

Rieber, H. (1977). Eine Ammonitenfauna aus der oberen Maiolica der Breggia-Schlucht (Tessin/Schweiz). *Eclogae Geologicae Helvetiae, 70*(3), 777–787.

Schenk, C. (1992). *Die Drusberg-und Schrattenkalk-Formation (Unterkreide) im helvetikum des Berner Oberlandes*. Ph.D. thesis, (pp. 169). University of Berne

Schlager, W., & J. Philip (1990), Cretaceous carbonate platforms. In: R. N. Ginsburg, B. Beaudoin (Eds.), *Cretaceous resources, events and rhythms: background and plans for research*. (vol., 304, pp. 173–195). NATO ASI Series C

Schroeder, R., Charollais, J.-J., & Conrad, M.-A. (1968). Essai de biozonation au moyen des orbitolinidae dans les calcaires urgoniens de la Haute-Savoie et de l'Ain, France. *Comptes rendus des séances de l'Académie des sciences. Série d, Sciences Naturelles, 267*, 390–393.

Schroeder, R., Clavel, B., Cherchi, A., Busnardo, R., Charollais, J., & Decrouez, D. (2002). Lignées phylétiques d'Orbitolinidés de l'intervalle Hauterivien supérieur-Aptien inférieur; leur importance stratigraphique. *Revue De Paléobiologie, 21*(2), 853–863.

Schroeder, R., Schenk, S., Cherchi, A., & Schwizer, B. (2007). Sur la présence de grands foraminifères d'âge aptien supérieur dans l'Urgonien de la Nappe du Wildhorn (Suisse centrale). *Note Préliminaire. Revue De Paléobiologie, 26*(2), 665–669.

Skelton, P. W. (2003). *The Cretaceous world* (p. 360). Cambridge: The Open University, Milton Keynes and Cambridge University Press.

Sprovieri, M., Coccioni, R., Lirer, F., Pelosi, N., & Lozar, F. (2006). Orbital tuning of a lower Cretaceous composite record (Maiolica Formation, central Italy). *Paleoceanography*. https://doi.org/10.1029/2005PA001224

Staeger, D. (1944). Geologie der Wilerhorngruppe zwischen Brienz und Lungern (Kantone Bern und Unterwalden). *Eclogae Geologicae Helvetiae, 37*, 99–188.

Stein, R., Rullkötter, J., Littke, R., Schaefer, R.G., & Welte, D.H. (1988). Organofacies reconstruction and lipid geochemistry of sediments from the Galicia Margin, northeast Atlantic. In: G. Boillot, E. L. Winterer, A.W. Meyer, J. Applegate, M. Baltuck, J.A. Bergen, M. C. Comas, K. Dunham, C. A. Evans, J. Girardeau, D. Goldberg, J. A. Haggerty, L. F. Jansa, J. A. Johnson, J. Kasahara, J-P. Loreau, E. Luna, M. Moullade, J.O. Ogg, M. Sarti, J. Thurow, & M.A. Williamson (Eds.), *Proceedings of the Ocean Drilling Program*. (vol., 103, pp. 567–585). Scientific Results

Stein, M., Arnaud-Vanneau, A., Adatte, T., Fleitmann, D., Spangenberg, J. E., & Föllmi, K. (2012a). Palaeoenvironmental and palaeoecological change on the northern Tethyan carbonate platform during the Late Barremian to earliest Aptian. *Sedimentology, 59*, 939–963.

Stein, M., Westermann, S., Adatte, T., Matera, V., Fleitmann, D., Spangenberg, J. E., & Föllmi, K. B. (2012b). Late Barremian–Early Aptian palaeoenvironmental change: The Cassis-La Bédoule section, southeast France. *Cretaceous Research, 37*, 209–222.

Studer, B. (1834). *Geologie der westlichen Schweizer-Alpen* (p. 420). Heidelberg und Leipzig: Gross.

Tajika, A., Kürsteiner, P., Pictet, A., Lehmann, J., Tschanz, K., Jattiot, R., & Klug, C. (2017). Cephalopod associations and palaeoecology of the Cretaceous (Barremian–Cenomanian) succession of the Alpstein, northeastern Switzerland. *Cretaceous Research, 70*, 15–54.

Talbi, R., Amri, A., Boujemaa, A., Gabtni, H., Spiller, R., & Levey, R. (2021). First evidence of the early cretaceous oceanic anoxic events (MBE and OAE1a) in the southern Tethyan margin (NE-Tunisia): Biostratigraphy and shale resource system. *Journal of Petroleum Exploration and Production, 11*, 1559–1575.

Tejada, M. L. G., Suzuki, K., Kuroda, J., Coccioni, R., Mahoney, J. J., Ohkouchi, N., Sakamoto, T., & Tatsumi, Y. (2009). Ontong Java plateau eruption as a trigger for the early Aptian oceanic anoxic event. *Geology, 37*, 855–858.

Tendil, A.J.-B., Frau, C., Léonide, P., Fournier, F., Borgomano, J. R., Lanteaume, C., Masse, J.-P., Massonat, G., & Rolando, J.-P. (2018). Platform-to-basin anatomy of a BarremianeAptian Tethyan carbonate system: New insights into the regional to global factors controlling the stratigraphic architecture of the Urgonian Provence platform (southeast France). *Cretaceous Research, 91*, 1–30.

Vermeulen, J. (2005). Boundaries, ammonite fauna and main subdivisions of the stratotype of the Barremian. In T. Adatte, A. Arnaud-Vanneau, H. Arnaud, M.-C. Blanc-Alétru, S. Bodin, E. Carrio-Schaffauser, K. Föllmi, A. Godet, M. C. Raddadi, J. Vermeulen (Eds.), *The hauterivian lower aptian sequence stratigraphy from jura platform to vocontian basin: A multidisciplinary approach*. Field-trip of the 7th International symposium on

the Cretaceous (September 1–4, 2005) (Vol. 7, pp. 147–166). Géologie Alpine, Colloques et excursions.
Weissert, H. (1981). The environment of deposition of black shales in the early Cretaceous: an ongoing controversy. In J. E. Warme, R. G. Douglas, & E. L. Winterer (Eds.), *The deep sea drilling project: a decade of progress* (Vol. 32, pp. 547–560). Society of Economic Paleontologists and Mineralogists, Special Publication.
Weissert, H., McKenzie, J., & Hochuli, P. (1979). Cyclic anoxic events in the early Cretaceous Tethys Ocean. *Geology, 7*(3), 147–151.
Wissler, L. (2001). *Response of early cretaceous sedimentary systems to perturbation in global carbon cycling: insights from stratigraphy, sedimentology and geological modelling*. Ph.D. thesis, ETH nr. 14380, Zürich, 129
Wissler, L., Funk, H., & Weissert, H. (2003). Response of early Cretaceous carbonate platforms to changes in atmospheric carbon dioxide levels. *Palaeogeography, Palaeoclimatology, Palaeoecology, 200*, 187–205.
Wissler, L., Weissert, H., Masse, J. P., & Bulot, L. G. (2002). Chemostratigraphic correlation of Barremian and lower Aptian ammonite zones and magnetic reversals. *International Journal of Earth Sciences, 91*, 272–279.
Yilmaz, I. O., Altimer, D., Tekin, U. K., & Ocakoglu, F. (2012). The first record of the "Mid-Barremian" Oceanic Anoxic Event and the Late Hauterivian platform drowning of the Bilecik platform, Sakarya Zone, western Turkey. *Cretaceous Research, 38*, 16–39.
Zerlauth, M., Ortner, H., Pomelly, H., Pfiffner, A. O., & Fügenschuh, B. (2014). Inherited tectonic structures controlling the deformation style: An example from the Helvetic nappes of the Eastern Alps. *Swiss Journal of Geosciences, 107*, 157–175.

Publisher's Note